Biochar (2022) 4:24
https://doi.org/10.1007/s42773-022-00149-y

REVIEW

Removal of toxic elements from aqueous environments using nano zero-valent iron- and iron oxide-modified biochar: a review

Sabry M. Shaheen[1,2,3] · Ahmed Mosa[4] · Natasha[5] · Hamada Abdelrahman[6] · Nabeel Khan Niazi[7] · Vasileios Antoniadis[8] · Muhammad Shahid[5] · Hocheol Song[9] · Eilhann E. Kwon[10] · Jörg Rinklebe[1,9]

Received: 26 November 2021 / Accepted: 23 March 2022

Abstract

Biochar (BC) has gained attention for removal of toxic elements (TEs) from aqueous media; however, pristine biochar often exhibits low adsorption capability. Thus, various modification strategies in BC have been developed to improve its removal capability against TEs. Nanoscale zero-valent iron (nZVI) and iron oxides (FeOx) have been used as sorbents for TE removal. However, these materials are prone to agglomeration and also expensive, which make their usage limited for large-scale applications. The nZVI technical demerits could be resolved by the development of BC-based composite sorbents through the loading of nZVI or FeOx onto BC surface. Nano zero-valent iron modified BC (nZVIBC), FeOx-modified BC (FeOxBC) have attracted attention for their capability in removing pollutants from the aqueous phases. Nonetheless, a potential use of nZVIBC and FeOxBC for TE removal from aqueous environments has not been well-realized or reviewed. As such, this article reviews: (i) the preparation and characterization of nZVIBC and FeOxBC; (ii) the capacity of nZVIBC and FeOxBC for TE retention in line with their physicochemical properties, and (iii) TE removal mechanisms by nZVIBC and FeOxBC. Adopting nZVI and FeOx in BC increases its sporptive capability of TEs due to surface modifications in morphology, functional groups, and elemental composition. The combined effects of BC and nZVI, FeOx or Fe salts on the sorption of TEs are complex because they are very specific to TEs. This review identified significant opportunities for research and technology advancement of nZVIBC and FeOxBC as novel and effective sorbents for the remediation of TEs contaminated water.

Keywords Feedstock · Engineered biochar · Toxic metal(loid)s · Biosorption · Wastewater remediation

✉ Jörg Rinklebe
rinklebe@uni-wuppertal.de

Sabry M. Shaheen
shaheen@uni-wuppertal.de

[1] Laboratory of Soil- and Groundwater-Management, Institute of Foundation Engineering, Water- and Waste-Management, School of Architecture and Civil Engineering, University of Wuppertal, Pauluskirchstraße 7, 42285 Wuppertal, Germany

[2] Department of Arid Land Agriculture, Faculty of Meteorology, Environment, and Arid Land Agriculture, King Abdulaziz University, Jeddah 21589, Saudi Arabia

[3] Department of Soil and Water Sciences, Faculty of Agriculture, University of Kafrelsheikh, Kafr El-Sheikh 33516, Egypt

[4] Soils Department, Faculty of Agriculture, Mansoura University, Mansoura 35516, Egypt

[5] Department of Environmental Sciences, COMSATS University Islamabad, Vehari Campus, Vehari 61100, Pakistan

[6] Soil Science Dept., Faculty of Agriculture, Cairo University, Giza 12613, Egypt

[7] Institute of Soil and Environmental Sciences, University of Agriculture Faisalabad, Faisalabad 38040, Pakistan

[8] Department of Agriculture Crop Production and Rural Environment, University of Thessaly, Fytokou Street, 384 46, Volos, Greece

[9] Department of Environment, Energy and Geoinformatics, University of Sejong, Guangjin-Gu, Seoul 05006, Republic of Korea

[10] Department of Earth Resources and Environmental Engineering, Hanyang University, Seoul 04763, Republic of Korea

Published online: 11 April 2022

1 Introduction

Contamination of toxic elements (TEs; such as Cr, As, U, V, Pb, Cd, and Hg) in aqueous environments has increased rapidly due to industrialization and lack of regulations, and can cause critical damage to all living organisms and ecosystem balance (Antoniadis et al. 2019; Shaheen et al. 2022a, b, c). Therefore, environmental contamination by TEs poses a major threat for human health (Rinklebe et al. 2019; Vasseghian et al. 2022). The effect of TEs on living organisms including human beings depends on their content and speciation (Shaheen et al. 2019a, b; Hussain et al. 2017; Natasha et al. 2021). Consequently, it is of great importance for humans and for the environmental protection to employ environment-friendly and economically viable means to efficiently remove/recover TEs from water (Sharma et al. 2021; Shaheen et al. 2019a, 2022a, b, c). Recently, the use of some byproducts has been tested for TE removal from water (Shaheen et al. 2013, 2015; Palansooriya et al. 2020; Wang et al. 2021a, b; Lashen et al. 2022). For efficient usage, these materials should be readily available, abundant, and thus cheap or free to obtain, easily biodegradable, and derived from renewable sources (Gupta et al. 2009; Ahmaruzzaman 2011; Singh et al. 2021a, b; Katiyar et al. 2021).

The two-fold effort of, firstly, achieving sustainable management of the hazardous materials, solid wastes, contaminated soils, and wastewater and, secondly, providing clean water, food, and environment makes significant contribution to meet the United Nations Sustainable Development Goals (Younis et al. 2021; Shaheen et al. 2022a, b, c). The safe recycling of biowastes for producing low-cost amendments and their use for remediation of water contaminated with TEs are priorities from agro-environmental and economic points of view.

Biochar (BC) is a carbon-rich product derived from pyrolysis of biomass (plant or animal residues) that could conform to all the requirements for TEs removal (Lehmann 2007, 2019; Lehmann and Joseph 2015). The attention of the scientific community concerning the use of BC as an environment-friendly amendment has increased in recent years due to its appealing benefits in various agro-environmental usages (Wu et al. 2019, 2020a, b, 2021a, b; Bolan et al. 2022; Lu et al. 2020). It is employed in waste management and treatment owing to its intrinsic porous structure (El-Naggar et al. 2021; Shaheen et al. 2022a, b, c; Amen et al. 2020; Pan et al. 2021). Several studies reported the effectiveness of BC for TEs removal from aqueous environments (Shaheen et al. 2019a, b; Singh et al. 2021a, b; Katiyar et al. 2021). Nonetheless, unmodified (alternatively termed "raw," "pristine," or "untreated") BC in reference to the commercially available sorbents exhibits low sorption efficiency (Liu et al. 2015; Faheem et al. 2016; Duan et al. 2019). In an effort to enhance the sorptive capability of BC, various modification schemes have been suggested (Wang et al. 2020; Xiong et al. 2021; Bolster 2021; Yang et al. 2022).

Impregnating BC with magnetic particles (e.g., Fe salts, Fe oxides (FeOx) and nano zero-valent iron (nZVI)), can produce magnetic BC (Gillingham et al. 2022). Some unmodified BC produced from feedstocks that contain high concentrations of Fe which successfully form magnetic particles through chemical changes induced by pyrolysis, may also be classed as magnetic BC (Reddy and Lee 2014; Rodriguez Alberto et al. 2019; Wurzer and Mašek 2021; Gillingham et al. 2022).

Although nano-sized zero-valent iron (nZVI) has been tested as sorbent for the removal of TEs and their immobilization (Hu et al. 2020; Liang et al. 2021; Tan et al. 2016), it is prone to agglomeration due to its steric effects among nanoscale particles and also expensive if applied alone, which makes its usage limited for large-scale applications (Tan et al. 2016). However, the limitations of nZVI could be overcome using BC-based composite adsorbents by means of the loading of nZVI, or similar agents like iron oxides (FeOx), onto the BC surface (Hu et al. 2020; Huang et al. 2019a; Faheem et al. 2016; Li et al. 2017). Nano zero-valent iron-modified biochar (nZVIBC) and FeOx-modified biochar (FeOxBC) have gained considerable attention for their capability in removing pollutants from aqueous environment as well as immobilizing soil pollutants (Wang et al. 2015a, b; Zou et al. 2016; Peng et al. 2017; Qian et al. 2017). As such, Tan et al. (2016) reported that a composite of BC and nanoscale oxides combined the advantages of both constituents and, thus, resulted in improved surface functional groups, pore properties, degradability, and were easily separable from the aqueous phase. Nevertheless, these composites are capable of removing contaminants from aqueous environments (Tan et al. 2016; Ahmaruzzaman 2021; Liang et al. 2021). As the preparation, characterization, and application of nZVIBC and FeOxBC have not been sufficiently reviewed, this detailed review aims at updating the readers with the state-of-the-art of the subject and improving their understanding of BC modification with nZVI and FeOx. Also, the sorption behavior and retention mechanisms of TEs onto nZVIBC and FeOxBC were compared to those of raw BC under various experimental conditions. Lastly, this review discusses the future opportunities and challenges for the production/use of nZVIBC and FeOxBC for TEs removal from waters.

2 Why nZVIBC and FeOxBC?

Despite that BC is an efficient sorbent, its removal efficiency for water pollutants is restricted for the following reasons: (i) BC has a relatively limited number of functional groups (particularly inorganic reactive groups) depending on the feedstock; (ii) BC has relatively low ion-exchange capacity, resulting in its inability to retain high contaminant concentrations (Tan et al. 2015); (iii) finely-sieved BC cannot be readily separated from the aqueous phase (Chen et al. 2011; Reddy and Lee 2014); (iv) net charge on BC surface is predominantly negative, therefore, anionic species like As, Cr(VI), Mo, P, Se, and V cannot be retained if no environment-mediated changes in BC net charge take place; (v) raw BC may increase water/soil pH, which triggers higher mobility of some anionic TEs like As, Mo, Se, and V; (vi) the high sorption capacity of aqueous contaminants is limited to a narrow range of solution pH (Chen et al. 2020); (vii) pristine BC has a low desorbability potential for sorbed ions (Mosa et al. 2020); and (viii) raw BC capability to retain contaminants is highly contingent on the raw feedstocks and the pyrolysis conditions (Tan et al. 2015, 2016). Consequently, apart from the raw BC, chemically modified/activated/engineered BCs have gained much attention due to their enhanced properties and multidimensional applications (Imran et al. 2020; Wu et al. 2017). Biochar properties can be enhanced by various pre-/post-modification techniques, such as coating with nZVI (Amen et al. 2020; Wen et al. 2021; Yang et al. 2021a, b, c). The high functionality of nZVI supports its applications for decontamination of TEs and chlorinated compounds (Mukherjee et al. 2016; Sun et al. 2020).

FeOx can also be used for improving physicochemical properties of raw BC. It could be due to their intrinsic high affinity for TEs, low cost, high specific capacitance, environmental compatibility, and remarkable structural versatility (Zou et al. 2016; Yang et al. 2021a, b, c). Nevertheless, the poor electrical conductivity and redox kinetics of FeOx hinder its electrochemical applications. To circumvent the noted limitations and increase a chance to use FeOx pseudo-capacitance, a common strategy is to integrate oxide materials onto highly conductive substrates, such as a carbon-rich material (BC) (Zou et al. 2016; Tan et al. 2016). This strategy creates hybrid capacitors with a large pseudo-capacitance in addition to the capacitance provided by the electrical double layer at the supporting electrode surface (Zou et al. 2016; Tan et al. 2016). In addition, this strategy contributes to acquiring large active surface area and good electrical connection (Liu et al. 2015).

Although nano-FeOx has a high affinity for TEs due to their surface hydroxyl groups, it tends to be aggregated in aqueous solutions (Zhou et al. 2014). Such aggregation makes its applicability rather problematic (Zhou et al. 2014). Such technical demerits have raised the interest for synthetic sorbents by merging nano-FeOx onto BC, aiming at creating a low-cost and environment-friendly sorbent, which would combine the advantages and decrease the costs, as compared to individual nano materials (Zhou et al. 2014). Indeed, deposition of nano-oxides onto the BC surface may reduce a chance in aggregation and the resultant component may be developed into a more homogenous structure than what would be obtained after physical mixture of the original materials. In addition, the impregnation of BC with FeOx and nano-oxides enhances the immobilization of toxic oxyanions in soils/water as FeOx retains oxyanions via anion exchange (Zou et al. 2016). Meanwhile, the impregnation of BC with FeOx or nZVI improves original BC physical and/or chemical properties that improve the TEs retention capacity (Tan et al. 2016).

3 Production technologies of nZVIBC and FeOxBC

With the recent advancement in chemical technology, the novel chemical methods have been introduced to synthesize nZVI. Most commonly, nZVI is produced using Fe salts such as $FeSO_4$ and a reducing agent, sodium borohydride ($NaBH_4$) as in Eq. 1 (Stefaniuk et al. 2016).

$$Fe\left(H_2O\right)_6^{3+} + 3BH_4^- + 3H_2O \rightarrow Fe^0 \downarrow +3B(OH)_3 + 10.5\,H_2 \quad (1)$$

Due to their high magnetic/redox properties, nZVI/FeOx tend to agglomerate, which indeed deteriorates their effectiveness as an environmental medium for pollutant removal (Wu et al. 2020a, b). Thus, to stabilize nZVI/FeOx and enhance its remediation efficiency, they are anchored on porous materials: the resultant materials possess the properties of both porous material and the nZVI/FeOx (Ahmad et al. 2018). The impregnation of nZVI/FeOx into BC led to excellent performance of the composite due to many facts such as the increased specific surface properties, the abundance of functional groups, and the high contaminant sorption efficiencies (Li et al. 2019a, b, c, d; Mu et al. 2017). The preparation protocols of nZVIBC and FeOxBC are slightly different from each other. Generally, the composites of iron oxide (such as FeOxBC) are prepared as follows: 2 g of biomass feedstock is added to Fe_3O_4 solution (0.5 g/500 mL) and the mixture is stirred for 24 h at the room temperature. The obtained FeOxBC are subjected to various washings (generally 5) with distilled water followed by drying in an oven at 80 °C to a constant weight (He et al. 2017). Two treatments are commonly used to synthesize nZVI-coated BC composites: (i) pre-treatment of raw feedstock and

(ii) post treatment to BC; both methods are summarized in Fig. 1. In some cases, nZVI is oxidized and hydrolyzed using dissolved oxygen in water to form FeOxBC composites (Zhang et al. 2020).

3.1 Pre-treatment

This method includes the impregnation of raw feedstock with Fe; alternatively, Fe is co-precipitated on biomass, and then in either case the feedstocks are pyrolyzed under various conditions. The resultant material is BC-based phase, which includes nZVI/FeOx particles into the pores of BC, as has been the case with $FeCl_3$-pretreated biomass reported elsewhere (Tan et al. 2016). Similarly, Yao et al. (2020) produced nZVI-coated BC with $FeCl_3$ on ground sorghum straw where the solid residues were first separated, dried, and then the $FeCl_3$-laden sorghum straw was thermolyzed at 800 °C. The resulting product was found to have exceptional surface properties.

3.2 Post-treatment

In this technique, the feedstock is pyrolyzed and then coated with nZVl metal. Most commonly, BC is submerged in $FeSO_4{\cdot}7H_2O$ solution and the reduction of iron from Fe^{2+} to Fe^0 is realized with dropwise addition of $NaBH_4$ by means of stirring. The resulting material is nZVI-coated BC that can be separated from the liquid phase and washed several times with ethanol (Table 1). Mitzia et al. (2020) synthesized nZVI-BC by mixing BC with nZVI suspension (nZVI:water = 1:1, w:w). After a sorption experiment, nZVI was found to be agglomerated with secondary and poorly-crystalline FeOx; however, agglomeration was lower than that of the original nZVI. The chemical reactions for the synthesis of nZVI-impregnated BC are as follows (Su et al. 2016b):

$$BC + Fe\left(H_2O\right)_6^{2+} \rightarrow BC - Fe\left(H_2O\right)_6^{2+} \quad (2)$$

$$BC - Fe\left(H_2O\right)_6^{2+} + 2BH_4 - \rightarrow Fe^0 - BC \downarrow + 2B(OH)_3 + 7H_2 \uparrow \quad (3)$$

A few studies have slightly modified the synthetic protocols for nZVIBC. Qian et al. (2017) agitated BC (0.2 g) in $FeSO_4$ solution at pH 4 for 24 h at 150 rpm. The solid part in the suspension was washed with ethanol and N_2 was purged for 1 h. The reduction reaction was conducted using potassium borohydride (KBH_4) and the synthesized nZVI-coated BC was separated from the aqueous phase using a magnet. Peng et al. (2017) synthesized the nZVIBC composites by sonicating a BC-$FeSO_4$ suspension for 1 h with N_2 supply. The reduction process was completed using $NaBH_4$ for 4 h under N_2. In an attempt to increase the binding/coating of nZVI on BC surface, Ahmad et al. (2020a, b) added chitosan (2% acetic acid) to the BC-$FeSO_4$ suspension (pH 6). To stabilize the reaction, 1.2% NaOH was added under stirring and N_2 purging and the reaction was continued for 1 h and the black particles were separated from the liquid phase.

Although most studies have used nZVI to fabricate nZVIBC composites, Iqbal et al. (2021) synthesized BC using the same method as described for nZVIBC composites using Mn salt and $NaBH_4$. Animal-derived BC can also be modified using nZVI to increase its ability for TE removal in water as reported by Liu et al. (2021a, Additional file 1:

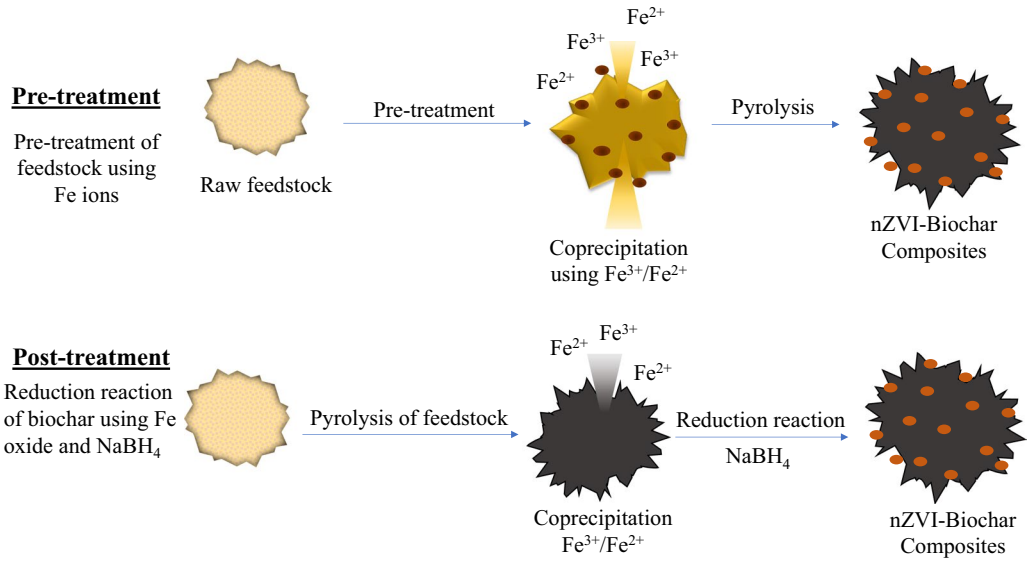

Fig. 1 Schematic diagram for the synthesis of nZVIBC/FeOxBC (Reproduced and modified from Tan et al. (2016) after a permission of the publisher)

Table 1 Synthesis of nano zero-valent iron-modified biochar (nZVIBC) and FeOx-modified biochar (FeOxBC)

Biochar feedstock	Pyrolysis temperature	Biochar mass used	Chemical used	Reducing agent	Degassing	Production ratio	Washing material	References
Bagasse	600 °C, 2 h	1 g	$FeSO_4{\cdot}7H_2O$ (4.9643 g in 50 mL)	$NaBH_4$ (30 mL, 2.8896 g/0.1% NaOH)	–	–	Ethanol	Li et al. (2020d)
Date palm	600 °C	56 g	$FeSO_4{\cdot}7H_2O$ (1 M, 100 mL)	$NaBH_4$ (2 M)	N_2	–	Ethanol	Ahmad et al. (2020a, b)
Sewage sludge	300 °C, 1 h	0.756 g	$FeSO_4{\cdot}7H_2O$ (250 mL, 0.054 M)	$NaBH_4$ (250 mL, 0.108 M)	N_2	1:1	Ethanol	Li et al. (2020a)
Corn stalk	800 °C, 2 h	–	$FeCl_3{\cdot}6H_2O$ (100 mL, 0.05 M)	$NaBH_4$ (100 mL, 0.2 M)	N_2	–	–	Li et al. (2020c)
Sewage sludge	300 ℃, 1 h	0.756	$FeSO_4{\cdot}7H_2O$ (50 mL, pH 5)	$NaBH_4$ (250 mL, 0.108 M)	N_2	–	Ethanol	Wei et al. (2020)
Wheat bran	500 °C, 3 h	1 g	$FeCl_3{\cdot}6H_2O$ (4.41 g/100 mL DI) (pH-5)	$NaBH_4$ (0.05 M)	N_2	1:1	Ethanol	Wan et al. (2019)
Corn stalk	600 °C, 2 h	1 g	$FeSO_4$ (100 mL 0.179 M)	$NaBH_4$ (120 mL, 0.3 M)	–	–	–	Zhu et al. (2019)
Palm	500 ℃, 8 h	1.68	$FeCl_3$ (30 mL 1 M)	$NaBH_4$ (200 mL, 0.6 M)	–	–	–	Jiang et al. (2018)
Mongolia	400 °C, 3 h	2 g	$FeSO_4{\cdot}7H_2O$ (500 mL, 0.075 M)	$NaBH_4$ (0.3 M, 300 mL)	N_2	–	Ethanol	Shang et al. (2017)
Saw dust	600 °C, 1 h	2.5 g	$FeSO_4{\cdot}7H_2O$ (2.474 g)	$NaBH_4$ (5 g/80 mL)	N_2	–	–	Peng et al. (2017)
Wheat straw	600 °C, 2 h	1.5 g	$FeSO_4{\cdot}7H_2O$ (100 mL, 0.25 M)	$NaBH_4$ (100 mL, 0.55 M)	-	1:1	Ethanol	Li et al. (2017)
Pine wood	600 °C, 1 h	5 g	$FeCl_3{\cdot}6H_2O$ (0.01 M)	$NaBH_4$ (5 g/80 mL)	Ar		Ethanol	Wang et al. (2017)
Rice husk	400 °C, 2 h	0.756 g	$FeSO_4{\cdot}7H_2O$ (0.054 M, 250 mL)	$NaBH_4$ (0.108 M)	N_2	1:1	Ethanol	Hussain et al. (2017)
Bagasse	600 °C, 2 h	0.42 g	$FeSO_4{\cdot}7H_2O$ (100 mL, 0.075 M)	$NaBH_4$ (0.3 M)	–	1:1	Acetone	Su et al. (2016b)
Bagasse	600 °C, 2 h	0.42 g	$FeSO_4{\cdot}7H_2O$ (100 mL, 0.075 M)	$NaBH_4$ (0.3 M)	–	1:1	Acetone/ethanol	Su et al. (2016a)
Rice hull	300 °C, 6 h	0.756 g	$FeSO_4{\cdot}7H_2O$ (0.054 M, pH 5.0)	$NaBH_4$ (250 mL, 0.108 M)	N_2	–	Ethanol	Yan et al. (2015)

Fig. S1). The pyrolysis conditions also affect the stability of nZVI-BC and its efficiency for removal of TEs. More specifically, in reference to conventional dry pyrolysis (moderate heating rates with long residence times), the wet pyrolysis process (known as hydrothermal carbonization) increases the stability of loaded Fe (94.54 vs. 98.59%) and the magnetization force (71.48 Oe and 1.31 emu g^{-1} vs. 125.76 Oe and 1.26 emu g^{-1} for coercivity and remanence, respectively) (Zhou et al. 2021). The hydrothermal carbonization or the wet pyrolysis process is generally carried out at a lower temperature (100–300 °C) via the heterogeneous reaction of BC and the nZVI solution in a reactor (Shaheen et al. 2022a, b, c). The wet pyrolysis has also been found to improve the maximum sorption capacity of Cr(VI) (83.02 mg g^{-1}) over

dry pyrolyzed Fe-loaded BC (70.79 mg g^{-1}); this was elucidated by the enhanced porosity/stability/magnetization, the abundance of active functional groups, and the specific surface area.

4 Characterization of Fe- and nZVI-coated BC

Coating of BC with nZVI offers enhanced BC adsorption capacities for TEs by improving surface morphology, functional group modification, and elemental composition in reference to the pristine one (Ahmad et al. 2019, 2020a, b; Fig. 2). Previously, Nguyen et al. (2019) found a heterogeneous structure (a structure with dissimilar components or elements, appearing irregular or variegated) of Fe-coated BC surface compared to the pristine, a feature that contributes to enhanced As retention. Similarly, FTIR analysis of nZVI-coated BCs confirmed the change in surface properties after modification (Fig. 2). These alterations in surface properties enhanced the sorption capacities for TEs (Ahmad et al. 2019, 2020a, b). The details of BC surface modification after coating with nZVI are discussed below.

4.1 Surface deposition of nZVI on biochar

The nano size of nZVI allows it to be dispersed onto BC, which can be identified and confirmed by SEM images and FTIR/XRD analyses. The XRD patterns of nZVIBC exhibit clear diffraction peak characteristics of nZVI, which evidences the synthesis of nZVIBC (Liu et al. 2021b). Yang et al. (2021b) reported that nZVI particles were agglomerated on BC to form spherical chain structures. Compared to nZVIBC, the starch-modified nZVIBC showed that nZVI was uniformly dispersed on surface with higher nZVI aggregation on nZVIBC than in the starch-modified nZVIBC. The SEM images of nZVI-coated corn straw BC revealed a uniform, uneven, granular and solidified covering of nZVI onto BC, and that nZVI particles were homogeneously distributed onto the BC surface and pores (Li et al. 2020b).

Moreover, Zhang et al. (2021) fabricated longan shell BC; as a raw material it was with block structure and irregular morphology but when coated, nZVI was reported to be evenly diffused on the BC surface. Furthermore, the characteristic diffraction peaks of XRD spectra of pristine BC and nZVI were found to remain in the nZVIBC material. This was a sign for the successful synthesis of nZVIBC that exhibited FeOx bands along with the original characteristic bands (OH, C=O, C–O), presumably deriving from the nZVI loading onto BC. With the movement into the more environment friendly approaches, "green" methods, i.e.,

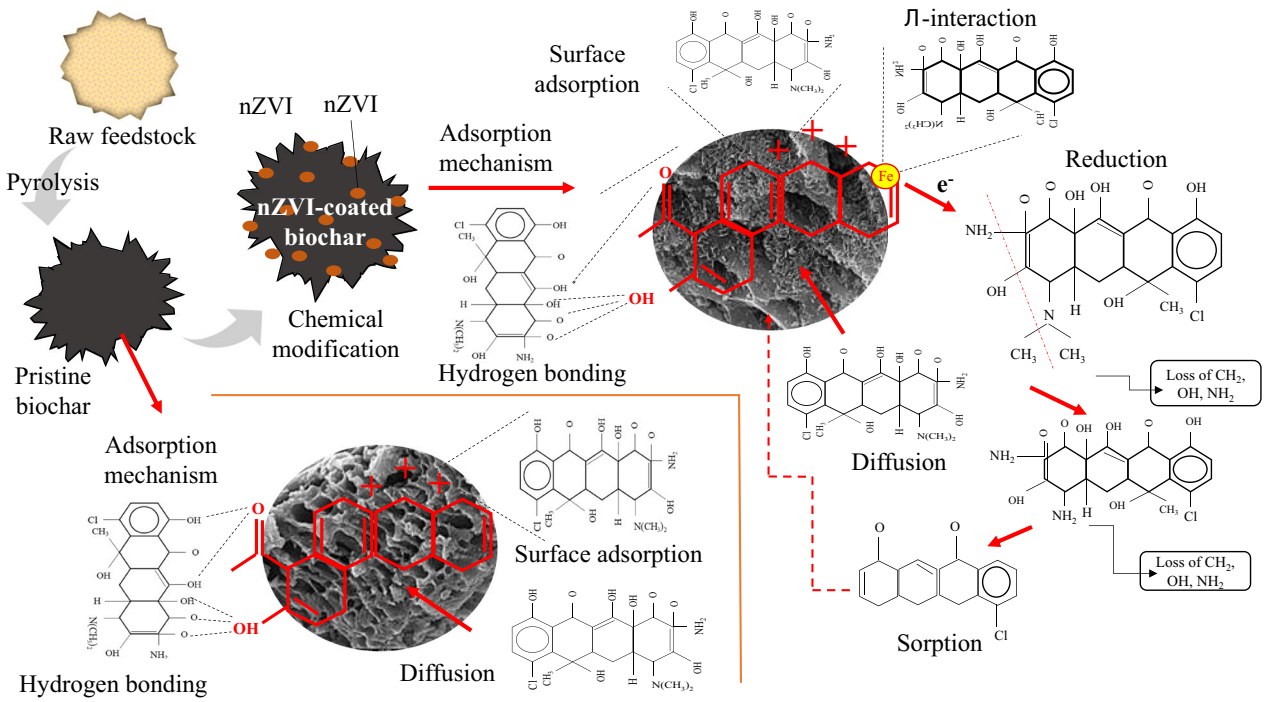

Fig. 2 Comparison of surface modification and adsorption mechanism of pristine and nZVIBC (Reproduced and modified from Ahmad et al. (2019, 2020a, b) after a permission of the publisher)

the use of plants, plant parts and/or plant extracts, has been employed to synthesize nanoscale particles. Indeed, it is a cheaper, faster and eco-friendly method. This method does not require high pressure, energy, or temperature, and it eliminates the need for large quantities of toxic chemicals (Deepak et al. 2019). Wang et al. (2021a) synthesized nZVI-loaded BC by "chemical" and "green" methods; however, both produced BCs had weak diffraction peaks of Fe_2O_3, Fe_3O_4 and Fe_3C, which proved the successful loading of nZVI onto BC. Still, the "green" nZVIBC was more resistant to oxidation with long-term reactivity than chemically synthesized nZVIBC.

In another work, the XRD patterns showed obvious characteristic peaks of nZVI at an angle ranging between 5 and 85° (Li et al. 2020b). The EDX/XRD patterns have also confirmed that the formed nZVIBC particles showed white color and were mainly composed of ZVI (Fan et al. 2020). Ma et al. (2021) synthesized nZVI-loaded BC by co-pyrolysis of feedstock with varying molarities (0.01, 0.05, 0.1 M) of K_2FeO_4. The XRD analysis indicated sharp diffraction peaks of ZVI, and the intensity of peaks increased linearly with the increase of molarity of K_2FeO_4, indicating that the crystallinity increased as the molarity of the Fe precursor increased.

4.2 Surface morphology

The chemical modification of BC with nZVI usually enhances its adsorption efficiency due to the enhanced surface area in line with the pore volume. It can also affect the chemical reactivity by increasing the electrostatic attraction, surface complexation, and the abundance of high-affinity adsorption sites, which maximize the capacity for TEs sorption. Several studies have characterized and compared the surface properties of pristine BC and nZVIBCs using SEM or the Brunauer–Emmett–Teller (BET) surface analyzer. Liu et al. (2021a) synthesized nZVI-coated BC and reported that the BET surface area increased from 84.3 $m^2\ g^{-1}$ for pristine BC to 509.2 $m^2\ g^{-1}$ for nZVI-coated BC. Also, Devi and Saroha (2015) reported a twofold increase in BC specific surface, micropore volume, pore diameter and total pore volume after coating with nZVI. Similarly, Wang et al. (2021a) reported a porous matrix with nZVI particles attached onto the BC surface, and they found that the "green"-synthesized nZVIBC exhibited a smaller degree of nZVI agglomeration and higher dispersibility of nZVI compared to chemically-synthesized nZVIBC.

Beside the increase in surface area, it is noteworthy that some studies also reported a diminished surface area of the nZVIBC composite after nZVI coating. For instance, Trinh et al. (2019) synthesized rice husk BC coated with nZVI at the two pyrolyzing temperatures (400 and 800 °C) and the BET analysis showed that after impregnation of BC with nZVI, surface area decreased from 141.2 to 132.4 $m^2\ g^{-1}$ (for pyrolysis at 400 °C) and from 213 to 181.9 $m^2\ g^{-1}$ (800 °C). Likewise, Li et al. (2019c) treated corn stover BC with $FeCl_3{\cdot}6H_2O$ to synthesize nZVI-coated BC and found a decreased surface area down to 224.8 $m^2\ g^{-1}$ from the original 339.6 $m^2\ g^{-1}$. Similarly, Zhang et al. (2021) reported that coating of BC with nZVI particles actually resulted in micropores being blocked, resulting in a 48% reduction in specific surface area. The increase/decrease of the surface area is highly contingent on the synthesis protocols, the feedstock used for biochar preparation, pyrolysis temperature, the relative amount of BC and Fe precursors. Ma et al. (2021) identified dosage, amount, and rate of Fe precursor addition as the decisive factors. They reported an increase in specific surface from 1018 to 1086 $m^2\ g^{-1}$ when the BC was treated with 0.01 M and 0.05 M K_2FeO_4. The specific surface area, however, decreased to 272 $m^2\ g^{-1}$ with increasing K_2FeO_4 dosage to 0.1 M due to the larger Fe content and the lower yield. The increase/decrease in surface area may be attributed to different chemical modifications taking place during composite synthesis, such as the release of volatiles from the biochar matrix. Similarly, the incorporation of nanoparticles facilitates the enlargement of the pores and hence increases the specific surface area (Zhu et al. 2015). However, the decreased specific surface area of nZVIBC is attributed to blocking of BC pore structure by nZVI particles (Zhu et al. 2019). It is also possible that the biochar pore structure gets collapsed by the chemical reactions during chemical modification.

4.3 Elemental composition

A biochar coated with nZVI exhibits changes in the elemental composition in reference to the pristine one. Qian et al. (2017) reported that BC without nZVI was abundant in organic (–OH, C=C, C–O), and inorganic reactive groups (Si–O–Si), whereas in the nZVI-coated BC, the typical bands of 1373 cm^{-1} (typical to Fe coating) were observed. Also, the FTIR spectra of pristine- and nZVI-BC revealed that there was significant difference in bands at ranges of 1710–1560 cm^{-1} and 470–1100 cm^{-1} due to nZVI loading onto BC. Wang et al. (2017) reported a 131-fold increase in Fe content (10.5) in nZVIBC composites compared to raw pinewood BC. Nevertheless, the concentrations of C and N were decreased by 15 and 5% in nZVIBC, as compared to control. Similarly, Mandal et al. (2020) reported that loading of BC with nZVI decreased Ca, K, C, Mg, Cu contents, while Fe increased. According to Wang et al. (2021a), an XRF (X-ray fluorescence) analysis revealed that in addition to the four basic elements (C, O, N, and H), Fe was the main element with

the largest percentage in nZVIBC. However, a remarkable reduction in C (40%) and O (42%) percentage in BC was also observed after nZVI treatment (Fan et al. 2020).

5 Applications of nZVIBC for removal of TEs in water

There are many studies reporting that nZVIBC exhibits the desirable surface properties and the high adsorption capacity for TEs as compared to the pristine BC (Fig. 3). The following subsection will present and discuss these studies in relation to specific TEs.

5.1 Chromium

Chromium exists in several oxidation states (−2 to +6), of which Cr(III) and Cr(VI) are the most prevalent and stable in natural environments (Zhang et al. 2019b). The toxicity of Cr(VI) is higher than Cr(III) by 1000 times for its strong oxidation capability, which causes several carcinogenic/mutagenic effects (Hu et al. 2021). Iron-loaded biochar showed high efficacy toward Cr(III) elimination from the aqueous environments. The dominant removal mechanism of Cr(III) by Fe-loaded biochar was the formation of nanoscale chromite ($FeCr_2O_4$) precipitates (Chen et al. 2020). In a previous work (Qiu et al. 2020), sludge derived biochar at 600 °C was served to support nZVI loading for efficient removal of Cr(III). The engineered nZVIBC recorded the sorption capacity of 28.89 mg g^{-1} through forming precipitates with Fe(II). The high capacity of nZVI to cause reduction has been explored in several investigations for Cr(VI) decontamination under the principle of redox chemistry between Fe and Cr (Fe^0/Fe^{2+} is −0.44 V and Cr(VI)/Cr(III) is 1.33 V) (Cheng et al. 2021; Xu et al. 2021). However, these nanoscale oxide particles showed a high tendency for agglomeration into larger-scale particles, which have low specific surface and, thus, limited the reduction capacity in sorbent–sorbate interactions (Huang et al. 2020). The utility of submerged aquatic plants for BC production has been investigated to support nZVI since their hollow structural matrix not only contains high C content but also high levels of cellulose, proteins, sugars, lipids and other active compounds that participate effectively in contaminant sequestration (Nautiyal et al. 2016). Figure 4 shows the schematic illustration of the Cr removal mechanisms using nZVIBC. The BC derived from *Egeria najas,* an aquatic plant with high reproductive capacity, was loaded with nZVI and was investigated for aqueous decontamination with Cr(VI) (Yi et al. 2020). The Cr(VI) maximum sorption onto the fabricated composite was 56.79 mg g^{-1}, and reached equilibrium after 30 min. Although the surface area of *Egeria najas* pristine BC was relatively low (22.17 m^2 g^{-1}), the impregnation with nZVI increased its surface area and consequently its surface adsorption as the BC adsorption of aqueous Cr(VI) was only 16.2%. The Cr(VI) adsorption by nZVI alone was 47.9%, due to the reduced surface area caused by particle aggregation. When the two materials were combined, Cr(VI) removal was 98.2%, as the high porosity of the carbonaceous matrix minimized aggregation of nZVI, and possibly coupled with electrochemical reduction of Cr(VI) into Cr(III)

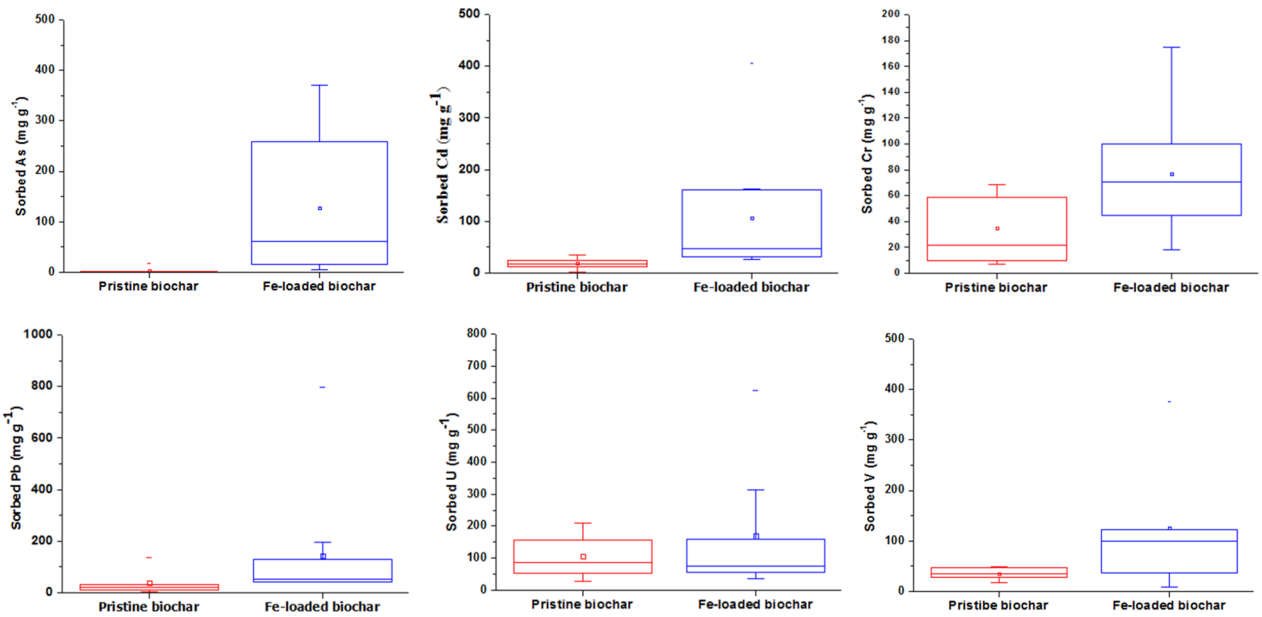

Fig. 3 Effect of Fe loading on the biochar sorption capacity for TEs in water

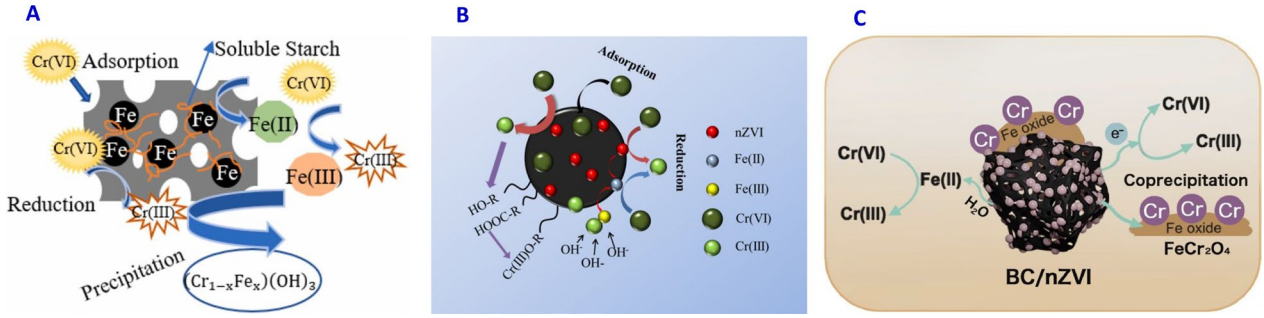

Fig. 4 Schematic illustration of Cr removal mechanisms using nZVIBC/FeOxBC

by the oxidation of Fe^0 into Fe^{2+}. Fan et al. (2019) synthesized nZVI-BC to explore its Cr(VI) removal efficiency, and its recyclability potential. Sorption capacity of Cr(VI) onto the synthesized composite reached 43.3 mg g^{-1}. Furthermore, the re-pyrolysis of spent BC showed a good efficacy to bind Cr(VI), with sorption maxima at 25.04, 8.04, and 7.46 mg g^{-1} with the first, second, and third pyrolysis cycle, respectively.

Organic stabilizers are encapsulated into nZVIBC composites to circumvent the potential agglomeration of nZVI (Liu et al. 2021b; Wu et al. 2021a, b). Soluble starch, a low-cost stabilizer rich in active functional groups, when loaded onto nZVIBC reduces the agglomeration and promote the crystallization of nZVI (Kumari and Dutta 2020). Yang et al. (2021a) reported a 99.67% removal efficiency of Cr(VI) ions by BC-stable starch loaded with nZVI (nZVI/SS/BC). It was deduced that a loading of soluble starch diminished the potential formation of secondary oxides, and increased the reducibility of Cr(VI) by Fe^0. Unexpectedly, the synthesized composite was able to persist and showed Cr(VI) removal efficiency at solution pH of 2.1–10.0. Similarly, the extract of pomegranate peel was tested to boost nZVIBC Cr(VI) removal (Wang et al. 2021b). The high polyphenolic content of pomegranate peel extract improved the reducibility potential of the fabricated composite, and Cr(VI) removal was ca. 100% within 90 min.

Three types of modified BCs (HCl-BC, KOH-BC and H_2O_2-BC) were synthesized from pyrolysis of corn stalk at 500 °C to prepare a supporter for nZVI (Dong et al. 2017). nZVI embedded onto HCl-BC showed the highest sorption capacity of Cr(VI), two times greater than the untreated one, due to the lower electronegativity and the higher surface area of HCl-BC, which reduced passivation of nZVI. Physical activation of BC was tried to enhance the interfacial affinity of FeOx with the surfaces of BC and increase the reducibility of Cr(VI). Iron-laden BC was produced by ball-milling (BM), and the performance of the produced BM-Fe-BC was investigated for Cr(VI) elimination from water (Zou et al. 2021). Ball milling maximized the specific surface area (~ 17.4% higher than Fe-BC), and improved the uniformity of FeOx distribution onto BC surfaces.

The reduction of Cr(VI) to Cr(III) has been repeatedly reported as a necessary step to allow the removal of Cr(VI). Qiu et al. (2021) studied the retention of Cr(VI) and Cr(III) by a sludge-derived BC (SDBC) modified with nZVI (NZVISDBC). They presumed that the matrix of BC could readily be an "electron shuttle mediator" facilitating the transfer of electrons from NZVI to sorbed Cr(VI). The reported kinetics of Cr(VI) removal indicated three distinct phases, each governed by the mechanisms of adsorption, reduction, and electrostatic attraction (see Additional file 1: Fig. S2).

As compared to other TEs, Cr shows different behavior with biochars including Fe-modified biochar, particularly under redox and pH changes. Reduction of Cr(VI) to Cr(III) followed by Cr(III) complexation is a major immobilization mechanism for Cr(VI) by BCs. The pH-dependent sorption of Cr(VI) in BCs increases under acidic conditions, which can be explained by the protonation of BC surface at low pH value, which favors the formation of ion-pair interaction mechanism between chromate (CrO_4^{2}) ions and the positively charged functional groups (Shaheen et al. 2019b). Also, the presence of electron donor functional groups (–C–OH, C–O, C–O–R) could promote sorption of Cr(VI) on biochar by sorption coupled reduction of Cr(VI) to Cr(III) in order to enable surface sorption (Shaheen et al. 2019a, b). The oxygen-containing compounds in BCs may be responsible for the reducing Cr(VI) to Cr(III) and its subsequent sorption by biochar (Shaheen et al. 2019b). Therefore, application of biochar in redox-sensitive media such as aquatic environments including wetlands might be an efficient tool to reduce and detoxify PTEs such as Cr(VI) (Yuan et al. 2017; Shaheen et al. 2019b).

5.2 Arsenic

Arsenic is a toxic metalloid and occurs in natural aquatic systems as arsine [As(− III)], non-valent species [As(0)], arsenite [As(III)] and arsenate [As(V)] (Alam et al. 2018). The aqueous

As species could be removed by means of co-precipitation with Fe oxyhydroxides and/or complexation onto the surface of nZVI by an outer layer of FeOx (Singh et al. 2021a, b). For instance, a Fe-modified BC, derived from rice straw at 500 °C, was tested for the removal of aqueous As(V), where the equilibrium was reached in 90 min, and the sorption maximum was 28.49 mg g^{-1} through complexation with Fe according to these proposed reactions (Nguyen et al. 2019):

$$FeOH + H_3AsO_4 \rightarrow FeH_2AsO_4 + H_2O \quad (4)$$

$$FeOH + H_2AsO_4^- \rightarrow FeH_2AsO_4^- + H_2O \quad (5)$$

$$FeOH + H_2AsO_4^{2-} \rightarrow FeH_2AsO_4^{2-} + H_2O \quad (6)$$

Also, pine wood BC fabricated at 600 °C was investigated to serve as a support for nZVI (Wang et al. 2017). nZVI-BC proved to have the high sorption capacity for As(V) irrespective of solution pH, and reached equilibrium within 1 h, where the sorption maximum at pH 4.1 was 124.5 mg g^{-1} with an active participation of the surface complexation mechanisms. This composite was also efficient to remove 100% of As(V) in the flowing conditions at 2.1 mg L^{-1} (as added concentration). The adsorption mechanisms were more effective by 8% under the anoxic conditions compared to the oxic ones due to Fe-oxidation. Under the anoxic conditions, however, the mechanisms of reduction became predominant alongside with the adsorption due to the presence of Fe^0. The oxidation of ZVI under the oxic/anoxic conditions can be attributed to the following reactions (Bang et al. 2005):

Under oxic conditions

$$2Fe^0 + O_2 + 4H^+ = 2Fe^{2+} + 2H_2O \quad (7)$$

$$4Fe^{2+} + 4H^+ + O_2 = 4Fe^{3+} + 2H_2O \quad (8)$$

Under anoxic conditions

$$Fe^0 + 2H^+ \rightarrow Fe^{2+} + H_2 \quad (9)$$

The mutual participation of Fe-containing substances, i.e. Fe^0, Fe^{2+} and FeOOH, and several organic species, e.g., dissolved organic matter, in the reduction of As(V) by sewage sludge BC (500 °C) supported by nZVI was also reported (Liu et al. 2021c). The maximum of sorption equaled 60.61 mg g^{-1} (at pH 2.0), and the soluble As was immobilized due to the formation of insoluble As–O–Fe species (Fig. 5; Liu et al. 2021c).

Although great attention has been paid to the feature of the specific surface area of BC, this criterion is insignificant when addressing As(III) decontamination by nZVIBC (Liu et al. 2021d). This understanding was based on testing BCs with varying specific surface areas (33.38–470.36 m^2 g^{-1}; Bakshi et al. 2018). It was found that BC electrochemical properties were more crucial to regulate the oxidation of BC for oxidizing highly toxic As(III) to the less toxic As(V). The work also showed that nZVI loading onto BC increased the average oxidation rate and the removal efficiency of As(V) in reference to nZVI (32% for composite vs. 27% for the sole nZVI; as for specific area, 306.5 for the composite *vs.* 192.7 mg g^{-1} for for the sole nZVI). This oxidation occurred by reactive oxygen species (ROS; i.e. Â·O^{2-}, OH and H_2O_2) generated under aerobic conditions through electron transfer

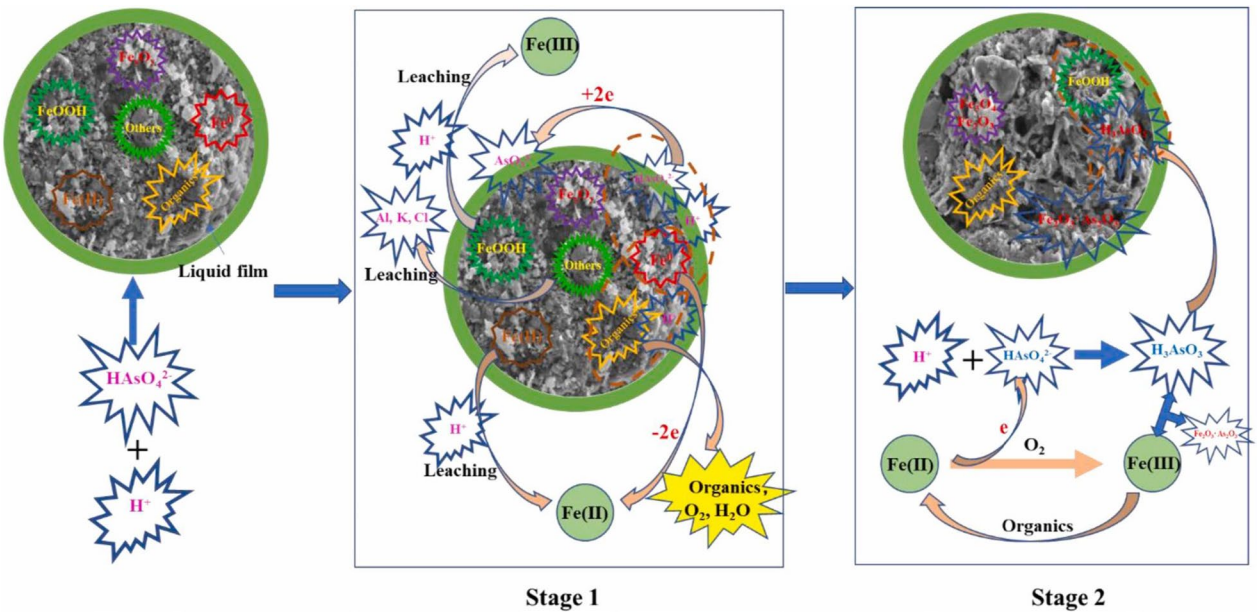

Fig. 5 Potential mechanisms of As(V) removal by nZVIBC/FeOxBC (Reproduced from Liu et al. (2021c) after a permission of the publisher)

from nZVI to H_2O_2. The surface quinone moieties have also been found to induce electron transfer between BC and nZVI, which promotes the origination of ROS (Â·O^{2-}, in particular) towards As(III) oxidation. In a study aimed to remove As(V) from drinking water, ZVIBC was prepared by the pyrolysis of red oak (RO) and switchgrass (SG) feedstocks and magnetite at 900 °C (Bakshi et al. 2018). The maximum sorption was 15.58 mg g^{-1} for ZVI/RO-BC and 7.92 mg g^{-1} for ZVI/SG-BC. The remediation mechanisms were suggested to be Fe^0 oxidization to Fe^{3+} and the simultaneous reduction of As(V) to As(III), followed by isomorphic substitution between As(III) and Fe(III) in α/γ-FeOOH.

In a study by Liu et al. (2020), As(III) removal from water by graphene-like BC (GBC) impregnated with nZVI was tested. The efficiency of nZVI-GBC for metal removal was significantly higher than GBC or nZVI (1.4 times). GBC promoted nZVI oxidation to form Fe oxyhydroxides and caused a 35% decrease of As(III) by converting it into As(V). Reactive oxygen species (ROS) were responsible for oxidizing As(III) to As(V) following the reaction of nZVI with dissolved oxygen to form H_2O_2, which reacts with Fe(II) to form ROS. Oxidation and surface complexation were revealed as the dominant mechanisms, while electrostatic binding also affected As(III) removal (Fig. 6).

Biochar could promote the reduction of As(V) to As(III). Arsenic species, including As(III) and As(V) can undergo redox reactions in the presence of strong oxidizing (e.g., FeOx) and reducing agents, such as Fe on the biochar surface. The redox changes can strongly affect the removal efficiency of Fe-modified BCs (such as nZVIBC and FeOxBC) for As from water (Amen et al. 2020; Bolan et al. 2022). The pivotal role of Fe-modified BCs in redox transformation and removal of As might be noticed due to the presence of active moieties on biochar. The reducers (electron donating functional groups such as phenolic groups) and oxidants (compounds accepting electrons such as quinones and aromatic groups) on the surface of Fe-modified BCs highly affect the redox-induced transformations of As and its immobilization/sorption in water (Amen et al. 2020; Bolan et al. 2022; Yang et al. 2022).

5.3 Mercury

Mercury is discharged from the flue gas of coal combustion in three main forms, i.e., solid-state particulate mercury (Hg^p; < 2%, wt), mercuric oxide (Hg^{2+}; < 15%, wt) and gaseous elemental mercury (Hg^0; > 85 wt.%; Tang et al. 2016). The Hg^p and Hg^{2+} species are easily eliminated by the traditional gas purification systems; however, Hg^0 has low solubility and high volatility and is thus difficult to eliminate (Shi et al. 2021). Activated carbon has been widely used in the gas purification systems of coal-fired power plants; however, its future application in industry is limited due to its high cost, limited sorption capacity at narrow range of temperatures, and low renewability potential (Tan et al. 2016). Biochar, impregnated with other materials, has attracted an interest for mercury removal in recent years. As such, novel Fe-BC composites were doped with Ce, Cu and Mn and compared with Fe-BC and pristine BC for removal of Hg^0 (Jia et al. 2021). Biochar doping with metals significantly improved the oxidation efficiency of Hg^0 compared with pristine BC, which showed minor oxidation capacity. Biochar doping with multiple elements was even more efficient than doping with a single element, and Hg^0 removal by

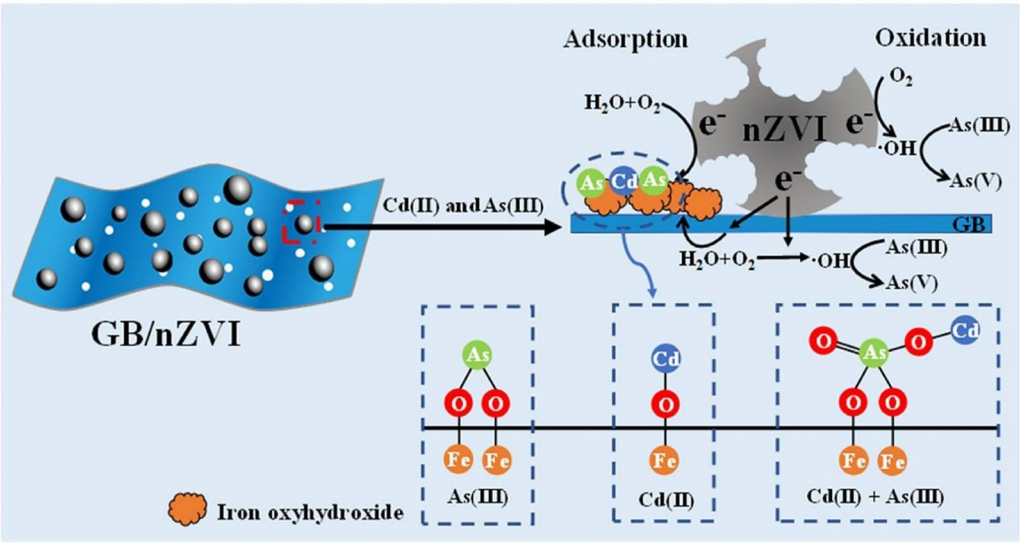

Fig. 6 The potential mechanisms of As(V) and Cd (II) removal by nZVIBC/FeOxBC. (Reproduced from Liu et al. (2020) after a permission of the publisher)

Fe-Ce-Mn-BC composite was significantly higher than those of Fe-BC by 13.3 times and of the pristine BC by 14.4 times.

The significantly higher ability of $FeCl_3$-modified sawdust BC (pyrolyzed at 500–800 °C) for the removal of Hg^0 in a simulated combustion flue gas as compared to the untreated BC has been reported by Yang et al. (2016). The produced $FeCl_3$-modified BC was 78% more efficient than the unmodified one, due to the fact that a coordination of Fe^{3+} in tetrahedral coordination [Fe^{3+}(t)] and lattice oxygen acted as active sorption/oxidizing sites for Hg^0. The integration of heteroatom dopants into Fe-BC composites might also increase the sorption capacity of the engineered composites due to the electron-withdrawal effect, which promotes sequestration of the transition elements. In a recent work, doping of Fe-BC with Mn maximized the sorption capacity of Hg^0 (4141 ng g^{-1}) over the undoped 10%-Fe based BC (2779 ng g^{-1}) and the unmodified BC (1912 ng g^{-1}; Jia et al. 2018). This noticeable increase by the modified BCs was caused by the chemisorption of Hg^0 into HgO and Hg-OM, however, the physisorption was apparently the only mechanism involved to the unmodified BC.

Unfortunately, few studies have been carried out to evaluate the effectiveness of Fe-BC composites on Hg^{2+} elimination. For example, banana peels were treated with Fe salts to produce Fe-modified BC (500 °C) for the efficient removal of Hg^{2+} (Oladipo et al. 2019). The porous structures, abundance of active functional groups, high magnetization (39.55 emu g^{-1}), and high specific surface of 323.2 m^2 g^{-1}, promoted Hg^{2+} sorption (83.4 mg g^{-1}) by the modified BC over the original BC (45.5 mg g^{-1}) at pH 6.0. The predominant mechanisms were ion exchange, Hg^{2+}–π stacking, electrostatic attraction and inner-sphere complexation. The future research on Hg^{2+} immobilization using Fe-BC composites should focus on dissolved organic materials derived from BC. Based on findings of Hg^{2+} sorption onto 36 types of BC, > 99% of sorbed Hg^{2+} was complexed by dissolved organic materials derived from BC (Liu et al. 2019). This high affinity between Hg^{2+} ions and dissolved organic materials was highly pronounced under low pyrolysis temperature and manures compared to high temperature and woody biomass (Liu et al. 2019).

5.4 Uranium

A tremendous increase of radionuclides (uranium (VI)) discharges into aquatic ecosystems has occurred due to the fast growth in nuclear power generations (Ma et al. 2020; Wollenberg et al. 2021). Due to its high surface reactivity, BC has been exploited for U(VI) elimination from water. A Fe-modified rice husk BC was used for U(VI) removal from water (Li et al. 2019a), where a relatively low sorption capacity (52.63 mg g^{-1} at pH 4.0) was realized via surface complexation and reduction into U(IV) as the main mechanisms. The U(VI) removal by the Fe-modified BC, prepared via the hydrothermal synthesis of FeOx particles, was about two times that of the unmodified BC (118 mg g^{-1} vs. 64 mg g^{-1}) due to the improved specific surface area, porosity and hydrophobicity that led to enhanced complexation and ion exchange (Wang et al 2018). Nevertheless, a significant decrease in the sorption capability of U(VI) was observed from the reusability of Fe-BC composite due to the leaching of Fe_3O_4. Another study pointed out to a slight increase in aqueous U(VI) sequestration by Fe_3O_4-modified BC, from the carbonization of hydrophyte biomass at 700 °C, (54.35 mg g^{-1} vs. 52.36 mg g^{-1} for the pristine BC), where inner-sphere complexation and reduction into U(IV) were proposed as the potential mechanisms toward U(VI) sequestration. Apparently, the high Si content in feedstock, e.g. rice husk, could improve the sorption capacity of U(VI) onto FeOx-BC composite (138.88 mg g^{-1}), with 99.8% removal of the initial U(VI), due to the enhanced specific surface area of the synthesized composite (62.88 m^2 g^{-1}; Sen et al. 2021).

These shortcomings of U(VI) sorption by Fe_3O_4-modified BC were addressed through oxidation of a fabricated composite, supported by pine needles as a precursor, by HNO_3 to produce Fe_3O_4-oxidized BC (Philippou et al. 2019). The sorption capacity of U(VI) onto Fe_3O_4-modified BC increased from 71.9 to 623.7 mg g^{-1}, with inner-sphere adsorption being the key sorption mechanism. Nevertheless, the re-used Fe_3O_4-loaded oxidized BC showed a remarkable reduction in sorption (from 99.5 to 87.2%) and desorption (from 99.6 to 62.6%) of U(VI), either by the loss of sorbed U(VI) or by the loss of the sorbent material during the regeneration cycles. Supporting BC with starch and nanoscale iron sulfide (SFeS-BC) has also been tested to improve the sorption capacity of U(VI) by Fe-loaded BC (Liu et al. 2021c). The SFeS increased the sorption capacity of U(IV) up to 76.32 mg g^{-1}, because of the mutual participation, reduction, electrostatic attraction, complexation, and precipitation mechanisms.

Biochar activation with Fe(0) towards U(IV) decontamination has been studied, taking into consideration the high reducibility of nZVI. Zhang et al. (2019a) tested nZVIBC composites from ferric chloride and ferric nitrate salts to produce $nZVI_{chloride}$-BC and $nZVI_{nitrtae}$-BC, respectively, and both composites showed a relatively low sorption capacity of U(IV) ions (34.82 and 55.14 mg g^{-1} for $nZVI_{chloride}$-BC and $nZVI_{nitrtae}$-BC, respectively), with the co-participation, sorption and reduction being the main mechanisms. Conversely, nZVI loading into BC (800 °C; longan shell) recorded a high sorption capacity of U(IV) ions (331.13 mg g^{-1}; Zhang et al. 2021). The reduction mechanism contributed significantly in U(VI) decontamination through the participation of Fe^0 and Fe^{2+} (converted to oxidized $Fe^{III}OOH$, $Fe^{III}{}_2O_3$ and $Fe^{II}Fe^{III}{}_2O_4$ species (Fig. 7).

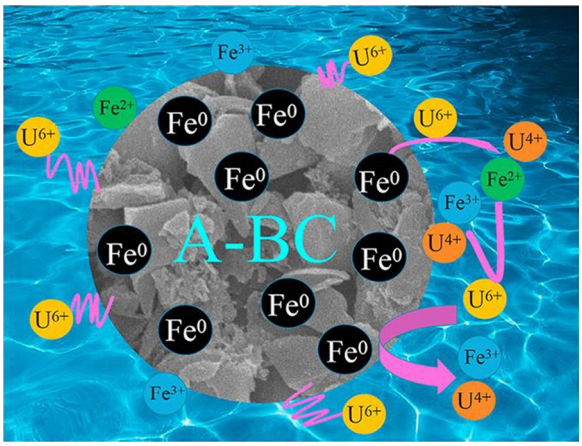

Fig. 7 Schematic illustration of U (VI) removal mechanism using nZVIBC/FeOxBC. (Reproduced from Zhang et al. (2021) after a permission of the publisher)

5.5 Vanadium (V)

The tracing of V could be a useful marker to monitor the potential release of TEs from the use of fossil fuels given the excessive release of V fingerprint from oil refinery and coal-fired power plants (Huang et al. 2021). The aquatic ecosystems are the most vulnerable to V accessibility including rivers (He et al. 2021; Klemt et al. 2020; Lin et al. 2013) and groundwater (Kong et al. 2020; Paradis et al. 2020; Shi et al. 2020). Still, studies on the effect of BC to sequester V are limited, due to the complicated reactions of V species under a wide range of pH values, and the low sorption capacity of BC towards V(V) and other anionic pollutants. Consequently, Fe-doped BCs might increase the effectiveness of BC toward V elimination from aquatic resources.

Corncob wastes were subjected to slow pyrolysis at 600 °C, and loaded with nZVI to produce nZVIBC that was used to treat water polluted with V(V) (Fan et al. 2020). The fabricated composite exhibited a high removal efficiency (46.2–48.5 mg g^{-1}) at pH 2.0–10.0, suggesting applicability of nZVIBC to remove V(V) under acidic/neutral/alkaline environments. The V(V) removal by nZVIBC occurred through the co-precipitation with Fe^{3+}, followed by the reduction by Fe^0 and Fe^{2+} to generate VO_2 (90%) and V_2O_5 (10%) as terminal species. Also, Ghanim et al. (2020) pyrolyzed a mixture of saw dust in the presence of red mud at 600 °C to produce a functionalized BC for efficient elimination of V(V) but the maximum sorption of V(V) onto the fabricated BC-red mud composite was relatively low (16.45 mg g^{-1}) at pH 3.5–5.5. However, the high ability of V(V) to be desorbed suggested the high reusability of this sorbent in subsequent regenerations. There was an evidently weak affinity between V(V) and the tested composite, which was attributed to the underlying mechanisms of electrostatic interaction and pore-entrapment which were weak.

5.6 Lead

Separation/disposing of Pb-laden BC still poses a tremendous challenge in the large-scale application (Zahedifar et al. 2021). For this purpose, scholars have strived to use modified BC composites with higher magnetization to enhance separation of Pb-laden BC from aqueous solutions. Huang et al. (2019b) prepared FeOxBC composite by doping Fe_3O_4 nanoparticles into amino-modified aerobic granular sludge BC for the efficient removal of Pb^{2+}. They found that the modification process improved the sorption capacity of synthesized BC (127.0 mg g^{-1} at pH 5.5 and equilibrium time of 360 min), with the electrostatic attraction, complexation and precipitation as the predominant mechanisms. Further, the developed FeOxBC composite showed a high reusability potential as the desorption efficiency of Pb^{2+} reached 88.14 mg g^{-1} after five cycles. Another study found that the removal capacity of Pb(II) by BC-supported nanoscale FeSBC composite was 88.06 mg g^{-1}, and the mechanisms involved were physisorption, ion exchange, electrostatic attraction, hydrogen bonding and precipitation (Chen and Qiu 2021). The FeSBC composite showed a high reusability potential as the removal capacity reached 58.12% in the fourth sorption–desorption cycle.

A hybrid BC was developed by grafting CeO_2–MoS_2 into Fe-modified BC (pyrolyzed at 600 °C) for Pb(II) removal (Li et al. 2019a, b, c, d). Hybridization improved the removal capacity of Pb(II) (263.6 mg g^{-1}). Hybridization further improved the renewability potential as the composite exhibited a good removal capacity (19.34 mg g^{-1}) after five sorption–desorption cycles. The underlying mechanisms for Pb(II) sorption onto the hybrid composite were electrostatic attraction, adsorption, complexation and Cπ–Pb(II) bond. Moreover, BC Fe-sodium alginate (Fe-SA-BC) showed a higher sorption capacity for Pb(II) (796.27 mg g^{-1}) than Fe-sodium alginate hydrogel (Fe-SA; 287.52 mg g^{-1}) and 900 °C-graphitic BC (84.42 mg g^{-1}) over pH range 2–6 (Zhao et al.2021).

Renewability and reusability of exhausted BC are of great importance to reduce the potential discharge of disposed materials into the ecosphere; however, this regeneration process might cause a reduction in the magnetization of the synthesized composites (Wang et al. 2015c). Sorption of Pb^{2+} onto the exhausted BC was comparable among six regeneration cycles, and the reduction was only observed in the first regeneration cycle (≃ 20.8%). Li et al. (2020a, b, c, d, e) produced a hydrophilic composite

consisting of BC embedded with nZVI (nZVI-HPB) for Pb removal. They found that nZVI-HPB was more efficient than the raw BC and the complexation and co-precipitation were invovled in metal removal (Fig. 8).

5.7 Cadmium

Biochar loading with Fe-species could progress the applicability of Cd(II) removal, and the renewability of the exhausted composite. For example, FeOxBC composite was fabricated from pine bark and $CoFe_2O_4$ by calcination at 950 °C and tested against Cd and Pb (Reddy and Lee 2014). The produced composite recorded a good sorption capacity over the range of solution pH (4–6), where the maximum sorption capacity of Cd^{2+} reached 14.96 mg g^{-1}. In another investigation, a synthesized nZVIBC composite was prepared through liquid-phase reduction of Fe(II) on pristine water hyacinth BC at 500 °C (Chen et al. 2019). The maximum sorption capacity of Cd^{2+} onto nZVIBC was enhanced (56.62 mg g^{-1} vs. 25.38 mg g^{-1} in pristine BC) with the the electrostatic adsorption, reduction, complexation and precipitation being the sorption mechanisms.

Khan et al. (2020) pyrolyzed maize straw at 600 and 800 °C, and the produced BC was further spiked with ferric nitrate to produce Fe-modified BC (Fe-BC600 and Fe-BC800). The resulting composites showed high Cd^{2+} immobilization capacity (28.71 and 46.90 mg g^{-1} for Fe-BC600 and Fe-BC800, respectively) compared to the conventional BCs (16.44 and 14.32 mg g^{-1} for BC600 and BC800, respectively) due to the increase in the specific surface area and in the abundance of reactive groups, beside the formation of inner-sphere complexations. The magnetic force of the developed composites (14.5 emu g^{-1} and 9.75 emu g^{-1}, respectively) motivated the ease of separating Cd-laden BC after sorption. Liu et al. (2020) used graphene-like BC (GBC) supported with nZVI to remove Cd from irrigation water and its efficiency was 1.7 times higher than GBC or nZVI alone. Surface complexation was identified as the predominant mechanism for Cd removal (Fig. 6).

5.8 Copper

FeOxBC was prepared under several pyrolysis temperatures (300–700 °C) for Cu^{2+} removal from wastewater (Phoungthong and Suwunwong 2020). It was reported that pyrolysis temperature had a minor effect on sorption and the maximum sorption ranged between 35.64 and 40.39 mg g^{-1}. Besides, surface complexation onto active functional groups (Fe–O stretching in particular), ion exchange (with K^+ and Zn^{2+}) and cation–π interaction could be the predominant mechanisms for Cu^{2+} immobilization. Similar results also reported that FeOxBC, derived from banana peels pyrolyzed at 500 °C, was more efficient than pristine BC for the removal of Cu^{2+} (75.9 mg g^{-1} vs.

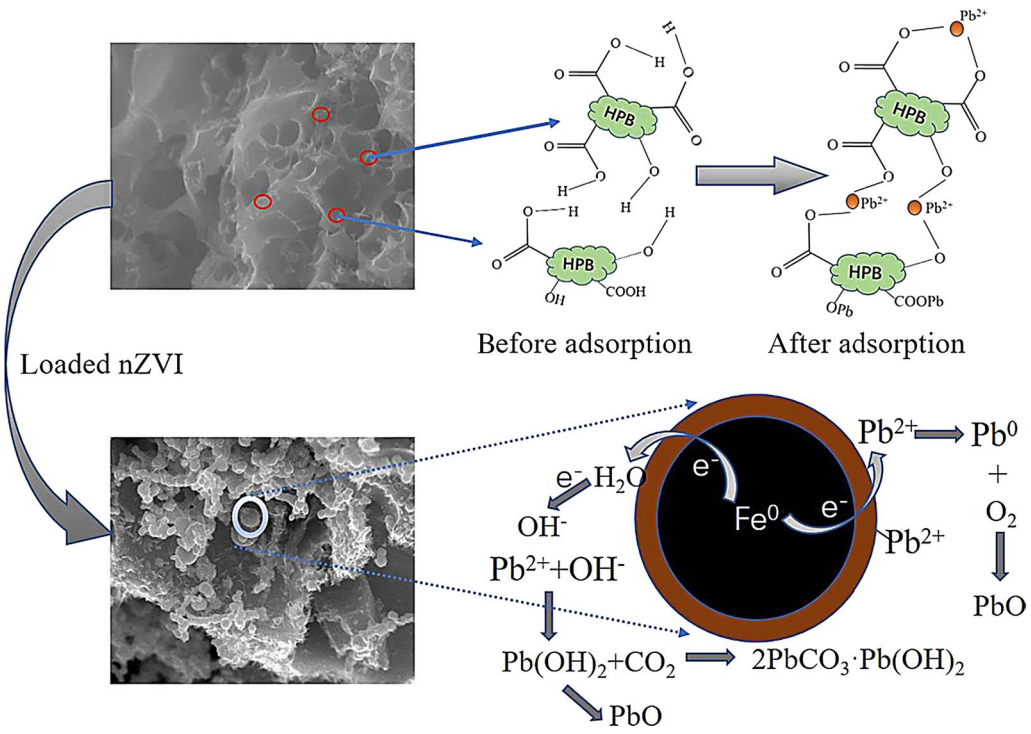

Fig. 8 Schematic diagram of possible Pb^{2+} adsorption mechanisms onto nZVIBC/FeOxBC (Reproduced from Li et al. (2020a, b, c, d, e) after a permission of the publisher)

44.9 mg g^{-1}) and Zn^{2+} (72.8 mg g^{-1} vs. 44.9 mg g^{-1}), due to its surface reactivity, which improved the active participation of several sorption mechanisms (M^{2+}–π stacking, ion exchange, adsorption and specific, inner-sphere, retention). In addition, the FeOxBC showed a high reusability potential with a high removal efficiency of Cu^{2+} (~ 89%) in the fifth regeneration cycle as compared to 97% in the first cycle.

Mandal et al. (2020) used corn stack BC modified with graphene and Fe^0 (CTBC-GO/nZVI) for Cu immobilization, where they found that nZVI-BC exhibited improved thermal stability relative to the graphene oxide-incorporated and untreated BC. CTBC-GO/nZVI was found to be more efficient in immobilizing soil Cu than the pristine BC or graphene oxide-modified BC (GOBC), where the mobile Cu decreased by more than 65% in CTBC-GO/nZVI, because the treatment resulted in the conversion of the accessible Cu into less bioavailable forms and thus reduced Cu toxicity (Fig. 9).

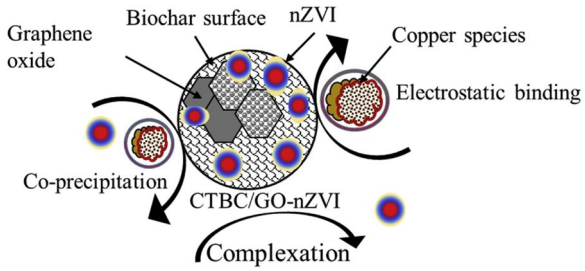

Fig. 9 Proposed mechanism for immobilization of copper from the soil by using corn stack biochar modified with nZVI (Reproduced from Mandal et al. (2020) after a permission of the publisher)

6 Conclusion and future needs

The coating of biochar (BC) surface with nZVI or FeOx increases its efficiency for toxic element (TE) sorption by altering surface morphology, functional group modification, and elemental composition. The conclusion of preparation and application of nZVIBC/FeOxBC for the removal mechanisms of TEs and environmental implications is illustrated in schematic diagram of Fig. 10. The combined effects of BC and nZVI/FeOx properties on TE sorption were indeed metal-specific. Using the nZVIBC and/or FeOxBc for retaining water TEs is indeed to overcome the disadvantages of the mono use of either BC and/or nZVI and to shift from the traditional and less-effective materials to the novel and highly effective materials. More attention is warranted to study the redox-mediated interaction between Fe-doped BCs and cationic/anionic TEs using advanced spectroscopy and microscopic techniques. Future research should also pay much attention to the potential utilization of Fe-doped BCs in oxyanions decontamination. As little is known about the fate of nanomaterials in ecosystem, especially under different biotic impacts, more consolidated research should evaluate the environmental fate of nZVI, their potential impacts on human health, and their impacts on the whole ecosystem

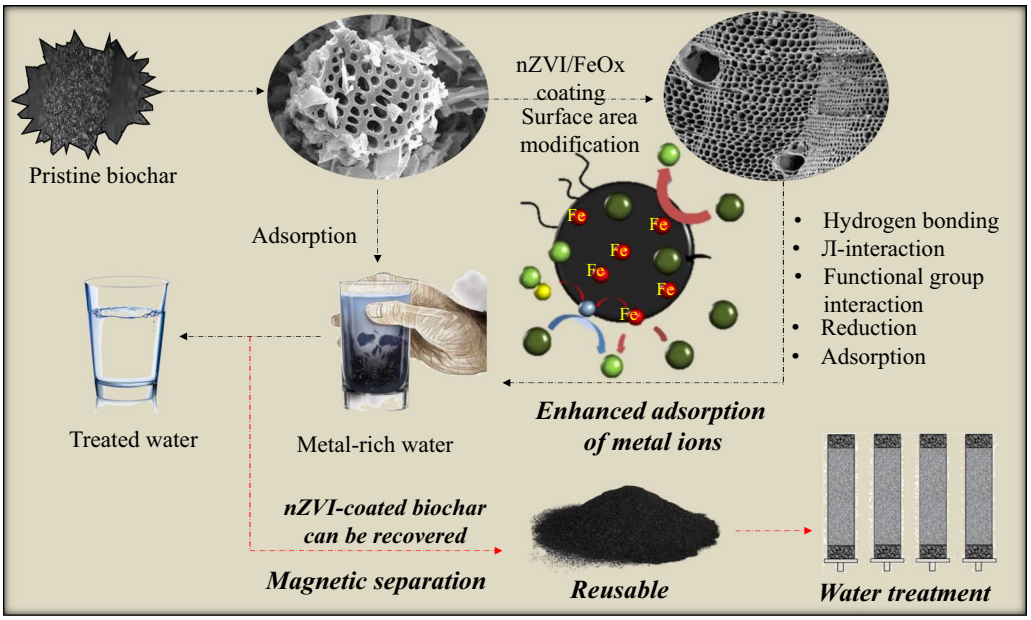

Fig. 10 Schematic diagram for the article's graphical abstract to conclude the preparation and application of nZVIBC/FeOxBC for TEs removal mechanisms and environmental implications

over time. Understanding and evaluating the cost effectiveness and feasibility of using nZVI in large scale is also relevant and important for broader application and optimization.

7 Highlights

- Removal of water toxic elements (TEs) using nZVI/FeOx-modified biochar is reviewed.
- Coating of biochar with nZVI/FeOx increased its sorption capacity for water TEs.
- Coating of biochar with nZVI/FeOx improved its surface activity.
- TEs sorption on nZVIBC/FeOxBC is complex and highly metal-specific.
- The review elucidates the nZVIBC/FeOxBC potential for cleaning contaminated water.

Supplementary Information The online version contains supplementary material available at https://doi.org/10.1007/s42773-022-00149-y.

Acknowledgements Not applicable.

Author contributions SS: Creating the idea, visualization, investigation, collecting review of literature, creating tables and figures, and writing the original draft. AM: Writing, creating tables and figures, review and editing, particularly Sect. 4. N: Writing, creating tables and figures, review and editing, particularly Sect. 3. HA: Writing-review and editing. NKN: Writing-review and editing. VA: Writing-review and editing. HS: Writing-review and editing. EEK: Writing-review and editing. JR: Visualization, writing-review and editing, and corresponding. All authors read and approved the final manuscript.

Funding No funding was received to assist with the preparation of this article.

Availability of data and materials Not applicable.

Declarations

Ethics approval and consent to participate Informed consent was obtained from all individual participants included in the study.

Consent to publish Authors are responsible for correctness of the statements provided in the manuscript.

The publication has been approved by all co-authors.

Competing interests The authors declare no potential conflict of interest. The authors declare that they have no known competing financial interests or personal relationships that could have appeared to influence the work reported in this paper.

References

Ahmad M, Ahmad M, Usman ARA, Al-Faraj AS, Abduljabbar AS et al (2018) Biochar composites with nano zerovalent iron and eggshell powder for nitrate removal from aqueous solution with coexisting chloride ions. Environ Sci Pollut Res 25:25757–25771

Ahmad M, Usman ARA, Rafique MI, Al-Wabel MI (2019) Engineered biochar composites with zeolite, silica, and nano-zerovalent iron for the efficient scavenging of chlortetracycline from aqueous solutions. Environ Sci Pollut Res Int 26(15):15136–15152

Ahmad M, Akanji MA, Usman ARA et al (2020a) Turning date palm waste into carbon nanodots and nano zerovalent iron composites for excellent removal of methylthioninium chloride from water. Sci Rep 10:16125

Ahmad M, Usman ARA, Hussain Q, Al-Farraj ASF, Tsang YF, Bundschuh J, Al-Wabel MI (2020b) Fabrication and evaluation of silica embedded and zerovalent iron composited biochars for arsenate removal from water. Environ Pollut 266:115256

Ahmaruzzaman Md (2011) Industrial wastes as low-cost potential adsorbents for the treatment of wastewater laden with heavy metals. Adv Colloid Interface 166:36–59

Ahmaruzzaman Md (2021) Biochar based nanocomposites for photocatalytic degradation of emerging organic pollutants from water and wastewater. Mater Res Bull 140:111262

Alam MA, Shaikh WA, Alam MO, Bhattacharya T, Chakraborty S, Show B, Saha I (2018) Adsorption of As (III) and As (V) from aqueous solution by modified *Cassia fistula* (golden shower) biochar. Appl Water Sci 8:198

Amen R, Bashir H, Bibi I, Shaheen S, Niazi N, Shahid M et al (2020) A critical review on arsenic removal from water using biochar-based sorbents: the significance of modification and redox reactions. Chem Eng J 396:125195

Antoniadis V, Shaheen SM, Levizou E, Shahid M, Niazi NK, Vithanage M, Ok YS, Bolan N, Rinklebe J (2019) A critical prospective analysis of the potential toxicity of trace element regulation limits in soils worldwide: Are they protective concerning health risk assessment? - A review. Environ Int 127:819–847. https://doi.org/10.1016/j.envint.2019.03.039

Bakshi S, Banik C, Rathke SJ, Lair DA (2018) Arsenic sorption on zero-valent iron-biochar complexes. Water Res 137:153–163

Bang S, Korfiatis GP, Meng X (2005) Removal of arsenic from water by zero-valent iron. J Hazard Mater 121:61–67

Bolan N, Hoang SA, Beiyuan J, Gupta S, Hou D, Karakoti A et al (2022) Multifunctional applications of biochar beyond carbon storage. Int Mater Rev. https://doi.org/10.1080/09506608.2021.1922047

Bolster CH (2021) Comparing unamended and Fe-coated biochar on removal efficiency of bacteria, microspheres, and dissolved phosphorus in sand filters. Biochar 3:329–338

Chen C, Qiu M (2021) High efficiency removal of Pb (ii) in aqueous solution by a biochar-supported nanoscale ferrous sulfide composite. RSC Adv 11:953–959

Chen B, Chen Z, Lv S (2011) A novel magnetic biochar efficiently sorbs organic pollutants and phosphate. Bioresour Technol 102:716–723

Chen L, Li F, Wei Y, Li G, Shen K, He HJ (2019) High cadmium adsorption on nanoscale zero-valent iron coated Eichhornia crassipes biochar. Environ Chem Lett 17:589–594

Chen M, He F, Hu D, Bao C, Huang Q (2020) Broadened operating pH range for adsorption/reduction of aqueous Cr(VI) using biochar from directly treated jute (*Corchorus capsularis* L.) fibers by H3PO4. Chem Eng J 381:122739

Cheng Y, Dong H, Hao T (2021) $CaCO_3$ coated nanoscale zero-valent iron (nZVI) for the removal of chromium (VI) in aqueous solution. Sep Purif Technol 257:117967

Deepak P, Amutha V, Kamaraj C, Balasubramani G, Aiswarya D, Perumal P (2019) Chapter 15—Chemical and green synthesis of nanoparticles and their efficacy on cancer cells. In: Shukla AK, Iravani S (eds) Green synthesis, characterization and applications of nanoparticles. Elsevier, Amsterdam, pp 369–387

Devi P, Saroha AK (2015) Simultaneous adsorption and dechlorination of pentachlorophenol from effluent by Ni–ZVI magnetic biochar composites synthesized from paper mill sludge. Chem Eng J 271:195–203

Dong H, Deng J, Xie Y, Zhang C, Jiang Z et al (2017) Stabilization of nanoscale zero-valent iron (nZVI) with modified biochar for Cr(VI) removal from aqueous solution. J Hazard Mater 332:79–86

Duan W, Oleszczuk P, Pan B et al (2019) Environmental behavior of engineered biochars and their aging processes in soil. Biochar 1:339–351

El-Naggar A, Shaheen S, Chang SX, Hou D, Ok YS, Rinklebe J (2021) Biochar surface functionality plays a vital role in (im) mobilization and phytoavailability of soil vanadium. ACS Sustain Chem Eng 9:6864–6874

Faheem YuH, Liu J, Shen J, Sun X, Li J, Wang L (2016) Preparation of MnOx-loaded biochar for Pb2+ removal: adsorption performance and possible mechanism. J Taiwan Inst Chem Eng 66:313–320

Fan Z, Zhang Q, Gao B, Li M, Liu C, Qiu Y (2019) Removal of hexavalent chromium by biochar supported nZVI composite: batch and fixed-bed column evaluations, mechanisms, and secondary contamination prevention. Chemosphere 217:85–94

Fan C, Chen N, Qin J, Yang Y, Feng C et al (2020) Biochar stabilized nano zero-valent iron and its removal performance and mechanism of pentavalent vanadium(V(V)). Colloids Surf A Physicochem Eng Asp 599:124882

Ghanim B, Murnane JG, O'Donoghue L, Courtney R, Pembroke JT, O'Dwyer TF (2020) Removal of vanadium from aqueous solution using a red mud modified saw dust biochar. J Water Process Eng 33:101076

Gillingham MD, Gomes RL, Ferrari R, West HM (2022) Sorption, separation and recycling of ammonium in agricultural soils: a viable application for magnetic biochar? Sci Total Environ 812:151440

Gupta VK, Carrott PM, Ribeiro Carrott ML, Suhas (2009) Low-cost adsorbents: growing approach to wastewater treatment—a review. Crit Rev Environ Sci Technol 39:783–842

He S, Zhong L, Duan J, Feng Y, Yang B, Yang L (2017) Bioremediation of wastewater by iron oxide-biochar nanocomposites loaded with photosynthetic bacteria. Front Microbiol 8:823

He Y, Huang D, Li S, Shi L, Sun W, Sanford RA, Fan H, Wang M, Li B, Li Y, Tang X, Dong Y (2021) Profiling of microbial communities in the sediments of Jinsha river watershed exposed to different levels of impacts by the Vanadium Industry, Panzhihua, China. Microb Ecol 82(3):623–637. https://doi.org/10.1007/s00248-021-01708-9

Hu B, Ai Y, Jin J, Hayat T, Alsaedi A, Zhuang L, Wang X (2020) Efficient elimination of organic and inorganic pollutants by biochar and biochar-based materials. Biochar 2:47–64. https://doi.org/10.1007/S42773-020-00044-4

Hu G, Long C, Hu L, Zhang Y, Hong S, Zhang Q, Zheng P, Su Z, Xu J, Wang L (2021) Blood chromium exposure, immune inflammation and genetic damage: Exploring associations and mediation effects in chromate exposed population. J Hazard Mater 425:127769

Huang Q, Song S, Chen Z, Jianrong HBC, Xiangke W (2019a) Biochar-based materials and their applications in removal of organic contaminants from wastewater: state-of-the-art review. Biochar 11(1):45–73. https://doi.org/10.1007/S42773-019-00006-5

Huang X, Wei D, Zhang X, Fan D, Sun X, Du B, Wei Q (2019b) Synthesis of amino-functionalized magnetic aerobic granular sludge-biochar for Pb(II) removal: adsorption performance and mechanism studies. Sci Total Environ 685:681–689

Huang X, Zhang F, Peng K, Liu J, Lu L, Li S (2020) Effect and mechanism of graphene structured palladized zero-valent iron nanocomposite (nZVI-Pd/NG) for water denitration. Sci Rep 10:1–11

Huang Y, Long Z, Zhou D, Wang L, He P, Zhang G et al (2021) Fingerprinting vanadium in soils based on speciation characteristics and isotope compositions. Sci Total Environ 791:148240

Hussain I, Li M, Zhang Y, Li Y, Huang S, Du X, Liu G, Hayat W, Anwar N (2017) Insights into the mechanism of persulfate activation with nZVI/BC nanocomposite for the degradation of nonylphenol. Chem Eng J 311:163–172

Imran M, Khan ZUH, Iqbal MM, Iqbal J et al (2020) Effect of biochar modified with magnetite nanoparticles and HNO_3 for efficient removal of Cr (VI) from contaminated water: a batch and column scale study. Environ Pollut 261:114231

Iqbal J, Shah NS, Sayed M et al (2021) Exploring the potential of nanozerovalent copper modified biochar for the removal of ciprofloxacin from water. Environ Nanotech Monit Manag 16:100604

Jia L, Fan BG, Yao YX, Han F, Huo RP, Zhao CW, Jin Y (2018) Study on the elemental mercury adsorption characteristics and mechanism of iron-based modified biochar materials. Energy Fuels 32:12554–12566

Jia L, Yu Y, Li ZP, Qin SN, Guo JR, Zhang YQ et al (2021) Study on the Hg0 removal characteristics and synergistic mechanism of iron-based modified biochar doped with multiple metals. Bioresour Technol 332:125086

Jiang X, Ouyang Z, Zhang Z, Yang C, Li X, Dang Z, Wu P (2018) Mechanism of glyphosate removal by biochar supported nanozero-valent iron in aqueous solutions. Colloids Surf A 547:64–72

Katiyar R, Patel AK, Nguyen TB, Singhania RR et al (2021) Adsorption of copper (II) in aqueous solution using biochars derived from *Ascophyllum nodosum* seaweed. Bioresour Technol 328:124829

Khan ZH, Gao M, Qiu W, Islam MS, Song Z (2020) Mechanisms for cadmium adsorption by magnetic biochar composites in an aqueous solution. Chemosphere 246:125701

Klemt WH, Kay ML, Wiklund JA, Wolfe BB, Hall RI (2020) Assessment of vanadium and nickel enrichment in Lower Athabasca River floodplain lake sediment within the Athabasca Oil Sands Region (Canada). Environ Pollut 265:114920

Kong X, Chen J, Tang Y, Lv Y, Chen T, Wang H (2020) Enhanced removal of vanadium(V) from groundwater by layered double hydroxide-supported nanoscale zerovalent iron. J Hazard Mater 392:122392

Kumari B, Dutta S (2020) Integrating starch encapsulated nanoscale zero-valent iron for better chromium removal performance. J Water Process Eng 37:101370

Lashen ZM, Shams MS, El-Sheshtawy HS et al (2022) Remediation of Cd and Cu contaminated water and soil using novel nanomaterials derived from sugar beet processing- and clay brick factory-solid wastes. J Hazard Mater 428:128205

Lehmann J (2007) A handful of carbon. Nature 447:143–144

Lehmann J (2019) Science-to-action through global and regional biochar networks. Biochar 1:337. https://doi.org/10.1007/s42773-019-00029-y

Lehmann J, Joseph S (2015) Biochar for environmental management: science, technology and implementation. Routlenge, London

Li H, Chen YQ, Chen S, Wang XL, Guo S, Qiu YF, Liu YD, Duan XL, Yu YJ (2017) Wheat straw biochar-supported nanoscale zerovalent iron for removal of trichloroethylene from groundwater. PLoS ONE 12:e0172337

Li M, Liu H, Chen T, Dong C, Sun Y (2019a) Synthesis of magnetic biochar composites for enhanced uranium(VI) adsorption. Sci Total Environ 651:1020–1028

Li R, Deng H, Zhang X, Wang JJ, Awasthi MK, Wang Q, Xiao R, Zhou B, Du J, Zhang Z (2019b) High-efficiency removal of Pb(II) and humate by a CeO2–MoS2 hybrid magnetic biochar. Bioresour Technol 273:335–340

Li S, You T, Guo Y, Yao S, Zang S, Xiao M et al (2019c) High dispersions of nano zero valent iron supported on biochar by one-step carbothermal synthesis and its application in chromate removal. RSC Adv 9:12428–12435. https://doi.org/10.1039/C9RA00304E

Li X, Huang L, Fang H, He G, Reible D, Wang C (2019d) Immobilization of phosphorus in sediments by nano zero-valent iron (nZVI) from the view of mineral composition. Sci Total Environ 694:133695

Li B, Wei D, Li Z, Zhou Y, Li Y, Huang C, Long J, Huang H, Tie B, Lei M (2020a) Mechanistic insights into the enhanced removal of roxsarsone and its metabolites by a sludge-based, biochar supported zerovalent iron nanocomposite: adsorption and redox transformation. J Hazard Mater 389:122091

Li P, Yu J, Huangfu Z, Chang J, Zhong C, Ding P (2020b) Applying modified biochar with nZVI/nFe 3 O 4 to immobilize Pb in contaminated soil. Environ Sci Pollut Res 27:24495–24506

Li S, Yang F, Li J, Cheng K (2020c) Porous biochar-nanoscale zerovalent iron composites: synthesis, characterization and application for lead ion removal. Sci Total Environ 746:141037. https://doi.org/10.1016/j.scitotenv.2020.141037

Li S, Yang F, Li J, Cheng K (2020d) Porous biochar-nanoscale zerovalent iron composites: synthesis, characterization and application for lead ion removal. Sci Total Environ 746:141037

Li Z, Sun Y, Yang Y, Han Y, Wang T, Chen J, Tsang DCW (2020e) Biochar-supported nanoscale zero-valent iron as an efficient catalyst for organic degradation in groundwater. J Hazard Mater 383:121240. https://doi.org/10.1016/j.jhazmat.2019.121240

Liang L, Xi F, Tan W, Meng X, Hu B, Wang X (2021) Review of organic and inorganic pollutants removal by biochar and biochar-based composites. Biochar 33(3):255–281. https://doi.org/10.1007/S42773-021-00101-6

Lin C, Wang J, Liu S, He M, Liu X (2013) Geochemical baseline and distribution of cobalt, manganese, and vanadium in the Liao River Watershed sediments of China. Geosci J 17:455–464

Liu W-J, Jiang H, Yu H-Q (2015) Development of Biochar-based functional materials: toward a sustainable platform carbon material. Chem Rev 115:12251–12285

Liu P, Ptacek CJ, Blowes DW (2019) Mercury complexation with dissolved organic matter released from thirty-six types of biochar. Bull Environ Contam Toxicol 103:175–180

Liu K, Li F, Cui J et al (2020) Simultaneous removal of Cd(II) and As(III) by graphene-like biochar-supportedbiocharsupported zero-valent iron from irrigation waters under aerobic conditions: synergistic effects and mechanisms. J Hazard Mater 395:122623

Liu K, Li F, Zhao X, Wang G, Fang L (2021a) The overlooked role of carbonaceous supports in enhancing arsenite oxidation and removal by nZVI: surface area versus electrochemical property. Chem Eng J 406:126851

Liu L, Zhao J, Liu X, Bai S, Lin H, Wang D (2021b) Reduction and removal of As(V) in aqueous solution by biochar derived from nano zero-valent-iron (nZVI) and sewage sludge. Chemosphere 277:130273

Liu R, Wang H, Han L, Hu B, Qiu M (2021c) Reductive and adsorptive elimination of U (VI) ions in aqueous solution by SFeS@ Biochar composites. Environ Sci Pollut Res 39:55176–55185

Liu W, Bai J, Chi Z, Ren L, Dong J (2021d) An in-situ reactive zone with xanthan gum modified reduced graphene oxide supported nanoscale zero-valent iron (XG-nZVI/rGO) for remediation of Cr(VI)-polluted aquifer: dynamic evolutions of Cr(VI) and environmental variables. J Environ Chem Eng 9:104987

Lu L, Yu W, Wang Y, Zhang K, Zhu X, Zhang Y, Wu Y, Ullah H, Xiao X, Chen B (2020) Application of biochar-based materials in environmental remediation: from multi-level structures to specific devices. Biochar 2:1–31. https://doi.org/10.1007/S42773-020-00041-7

Ma M, Wang R, Xu L, Xu M, Liu S (2020) Emerging health risks and underlying toxicological mechanisms of uranium contamination: lessons from the past two decades. Environ Int 145:106107

Ma D, Yang Y, Liu B, Xie G, Chen C, Ren N, Xing D (2021) Zero-valent iron and biochar composite with high specific surface area via K2FeO4 fabrication enhances sulfadiazine removal by persulfate activation. Chem Eng J 408:127992

Mandal S, Pu S, He L, Ma H, Hou D (2020) Biochar induced modification of graphene oxide & nZVI and its impact on immobilization of toxic copper in soil. Environ Pollut 259:113851

Mitzia A, Vítková M, Komárek M (2020) Assessment of biochar and/or nano zero-valent iron for the stabilisation of Zn, Pb and Cd: a temporal study of solid phase geochemistry under changing soil conditions. Chemosphere 242:125248

Mosa A, El-Ghamry A, Tolba M (2020) Biochar-supported natural zeolite composite for recovery and reuse of aqueous phosphate and humate: batch sorption–desorption and bioassay investigations. Environ Technol Innov 19:100807

Mu Y, Jia F, Ai Z, Zhang L (2017) Iron oxide shell mediated environmental remediation properties of nano zero-valent iron. Environ Sci Nano 4:27–45

Mukherjee R, Kumar R, Sinha A, Lama Y, Saha AK (2016) A review on synthesis, characterization, and applications of nano zero valent iron (nZVI) for environmental remediation. Crit Rev Environ Sci Technol 46:443–466

Natasha SM, Khalid S, Bibi I, Naeem MA, Niazi NK et al (2021) Influence of biochar on trace element uptake, toxicity and detoxification in plants and associated health risks: a critical review. Crit Rev Environ Sci Technol 1:41

Nautiyal P, Subramanian KA, Dastidar MG (2016) Adsorptive removal of dye using biochar derived from residual algae after in-situ transesterification: alternate use of waste of biodiesel industry. J Environ Manag 182:187–197

Nguyen TH, Pham TH, Nguyen Thi HT et al (2019) Synthesis of iron-modified biochar derived from rice straw and its application to arsenic removal. J Chem. https://doi.org/10.1155/2019/5295610

Oladipo AA, Ahaka EO, Gazi M (2019) High adsorptive potential of calcined magnetic biochar derived from banana peels for Cu^{2+}, Hg^{2+}, and Zn^{2+} ions removal in single and ternary systems. Environ Sci Pollut Res 26:31887–31899

Palansooriya KN, Shaheen SM, Chen SS, Tsang DCW, Hashimoto Y, Hou D, Bolan NS, Rinklebe J, Ok YS (2020) Soil amendments for immobilization of potentially toxic elements in contaminated soils: A critical review. Enviro Int 134:105046. https://doi.org/10.1016/j.envint.2019.105046

Pan X, Gu Z, Chen W, Li Q (2021) Preparation of biochar and biochar composites and their application in a Fenton-like process

for wastewater decontamination: a review. Sci Total Environ 754:142104
Paradis CJ, Johnson RH, Tigar AD, Sauer KB, Marina OC, Reimus PW (2020) Field experiments of surface water to groundwater recharge to characterize the mobility of uranium and vanadium at a former mill tailing site. J Contam Hydrol 229:103581
Peng X, Liu X, Zhou Y, Peng B, Tang L, Luo L et al (2017) New insights into the activity of a biochar supported nanoscale zerovalent iron composite and nanoscale zero valent iron under anaerobic or aerobic conditions. RSC Adv 7:8755–8761
Philippou K, Anastopoulos I, Dosche C, Pashalidis I (2019) Synthesis and characterization of a novel Fe3O4-loaded oxidized biochar from pine needles and its application for uranium removal. Kinetic, thermodynamic, and mechanistic analysis. J Environ Manag 252:109677
Phoungthong K, Suwunwong T (2020) Magnetic biochar derived from sewage sludge of concentrated natural rubber latex (CNRL) for the removal of Al^{3+} and Cu^{2+} ions from wastewater. Res Chem Intermed 46:385–407
Qian L, Zhang W, Yan J, Han L, Chen Y, Ouyang D, Chen M (2017) Nanoscale zero-valent iron supported by biochars produced at different temperatures: synthesis mechanism and effect on Cr (VI) removal. Environ Pollut 223:153–160
Qiu Y, Zhang Q, Gao B, Li M et al (2020) Removal mechanisms of Cr(VI) and Cr(III) by biochar supported nanosized zero-valent iron: Synergy of adsorption, reduction and transformation. Environ Pollut 265(Part B):115018
Reddy D, Lee SM (2014) Magnetic biochar composite: facile synthesis, characterization, and application for heavy metal removal. Colloids Surf A Physicochem Eng Asp 454:96–103
Rinklebe J, Antoniadis V, Shaheen SM, Rosche O, Altermann M (2019) Health risk assessment of potentially toxic elements in soils along the Central Elbe River, Germany. Environ Int 126:76–88
Rodriguez Alberto D, Stojak Repa K, Hegde S, Miller CW, Trabold TA (2019) Novel production of magnetite particles via thermochemical processing of digestate from manure and food waste. IEEE Magn Lett 10:1–5
Sen K, Mishra D, Debnath P, Mondal A, Mondal NK (2021) Adsorption of uranium (VI) from groundwater by silicon containing biochar supported iron oxide nanoparticle. Bioresour Technol Rep 14:100659
Shaheen SM, Eissa F, Ghanem G, Gamal El-Din H, Al-Anany F (2013) Heavy metals removal from aqueous solutions and wastewaters by using various byproducts. J Environ Manag 128:514–521
Shaheen SM, Eissa F, Ghanem G, Gamal El-Din H, Al-Anan F (2015) Metal ion removal from wastewaters by sorption on activated carbon, cement kiln dust, and sawdust. Water Environ Res 87(6):506–515. https://doi.org/10.2175/106143015X14212658614630
Shaheen SM, Niaz NK, Hassan NE, Bibi I, Wang H, Tsang DC, Ok YS, Bolan N, Rinklebe J (2019a) Wood-based biochar for the removal of potentially toxic elements in water and wastewater: a critical review. Int Mater Rev 64:216–247
Shaheen SM, El-Naggar A, Jianxu Wang J, Hassan NEE et al (2019b) Chapter 14—Biochar as an (Im)mobilizing agent for the potentially toxic elements in contaminated soils. In: Ok YS, Tsang DCW, Bolan N, Novak JM (eds) Biochar from biomass and waste. Elsevier, Amsterdam, pp 255–274
Shaheen SM, Antoniadis V, Shahid M, Yang Y, Abdelrahman H, Zhang T, Hassan NE, Bibi I, Niazi NK, Younis SA, Almazroui M, Tsang Y, Sarmah A, Kim H, Rinklebe J (2022a) Sustainable applications of rice feedstock in agro-environmental and construction sectors: a global perspective. Renew Sustain Energy Rev 153:111791. https://doi.org/10.1016/j.rser.2021.111791
Shaheen SM, Natasha A, Mosa A, El-Naggar A, Faysal Hossain M, Abdelrahman H, Khan Niazi N, Shahid M, Zhang T, Fai Tsang Y, Trakal L, Wang S, Rinklebe J (2022b) Manganese oxide-modified biochar: production, characterization and applications for the removal of pollutants from aqueous environments—a review. Bioresour Technol 346:126581
Shaheen SM, Antoniadis V, Shahid M, Yang Y et al (2022c) Sustainable applications of rice feedstock in agro-environmental and construction sectors: a global perspective. Renew Sustain Energy Rev 153:111791
Shang J, Zong M, Yu Y, Kong X, Du Q, Liao Q (2017) Removal of chromium (VI) from water using nanoscale zerovalent iron particles supported on herb-residue biochar. J Environ Manage 197:331–337. https://doi.org/10.1016/j.jenvman.2017.03.085
Sharma P, Tripathi S, Chandra R (2021) Highly efficient phytoremediation potential of metal and metalloids from the pulp paper industry waste employing *Eclipta alba* (L) and *Alternanthera philoxeroide* (L.): biosorption and pollution reduction. Bioresour Technol 319:124147
Shi C, Cui Y, Lu J, Zhang B (2020) Sulfur-based autotrophic biosystem for efficient vanadium (V) and chromium (VI) reductions in groundwater. Chem Eng J 395:124972
Shi Q, Zhang X, Shen B, Ren K, Wang Y, Luo J (2021) Enhanced elemental mercury removal via chlorine-based hierarchically porous biochar with $CaCO_3$ as template. Chem Eng J 406:126828
Singh E, Kumar A, Mishra R, You S et al (2021a) Pyrolysis of waste biomass and plastics for production of biochar and its use for removal of heavy metals from aqueous solution. Bioresour Technol 320:124278
Singh P, Pal P, Mondal P, Saravanan G, Nagababu P, Majumdar S, Labhsetwar N, Bhowmick S (2021b) Kinetics and mechanism of arsenic removal using sulfide-modified nanoscale zerovalent iron. Chem Eng J 412:128667
Stefaniuk M, Oleszczuk P, Ok YS (2016) Review on nano zerovalent iron (nZVI): from synthesis to environmental applications. Chem Eng J 287:618–632
Su H, Fang Z, Tsang PE, Fang J, Zhao D (2016a) Stabilisation of nanoscale zero-valent iron with biochar for enhanced transport and in-situ remediation of hexavalent chromium in soil. Environ Pollut 214:94–100
Su H, Fang Z, Tsang PE, Zheng L, Cheng W, Fang J, Zhao D (2016b) Remediation of hexavalent chromium contaminated soil by biochar-supported zero-valent iron nanoparticles. J Hazard Mater 318:533–540
Sun Y, Zheng F, Wang W, Zhang S, Wang F (2020) Remediation of Cr (VI)-contaminated soil by nano-zero-valent iron in combination with biochar or humic acid and the consequences for plant performance. Toxics 8:26
Tan XF, Liu YG, Zeng G, Wang X, Hu X, Gu Y, Yang Z (2015) Application of biochar for the removal of pollutants from aqueous solutions. Chemosphere 125:70–85
Tan X-f, Liu Y-g, Gu Y-l, Xu Y et al (2016) Biochar-based nano-composites for the decontamination of wastewater: a review. Bioresour Technol 212:318–333
Tang S, Wang L, Feng X, Feng Z, Li R et al (2016) Actual mercury speciation and mercury discharges from coal-fired power plants in Inner Mongolia, Northern China. Fuel 180:194–204
Trinh B-S, Le PT, Werner D, Phuong NH, Luu TL (2019) Rice husk biochars modified with magnetized iron oxides and nano zero valent iron for decolorization of dyeing wastewater. Processes 7:660
Vasseghian Y, Almomani F, El Dragoi N (2022) Health risk assessment induced by trace toxic metals in tap drinking water: condorcet principle development. Chemosphere 286(Part 2):131821

Wan Z, Cho D-W, Tsang DCW, Li M, Sun T, Verpoort F (2019) Concurrent adsorption and micro-electrolysis of Cr(VI) by nanoscale zerovalent iron/biochar/Ca-alginate composite. Environ Pollut 247:410–420. https://doi.org/10.1016/j.envpol.2019.01.047

Wang H, Gao B, Wang S, Fang J, Xue Y, Yang K (2015a) Removal of Pb (II), Cu (II), and Cd (II) from aqueous solutions by biochar derived from $KMnO_4$ treated hickory wood. Bioresour Technol 197:356–362

Wang S, Gao B, Li Y, Mosa A, Zimmerman AR, Ma LQ, Harris WG, Migliaccio KW (2015b) Manganese oxide-modified biochars: preparation, characterization, and sorption of arsenate and lead. Bioresour Technol 181:13–17

Wang S-y, Tang Y-k, Chen C, Wu J-t, Huang Z, Mo Y-y, Zhang K-X, Chen J-b (2015c) Regeneration of magnetic biochar derived from eucalyptus leaf residue for lead(II) removal. Bioresource Technol 186:360–364

Wang S, Gao B, Li Y, Creamer AE, He F (2017a) Adsorptive removal of arsenate from aqueous solutions by biochar supported zerovalent iron nanocomposite: batch and continuous flow tests. J Hazard Mater 322:172–181

Wang S, Guo W, Gao F, Wang Y, Gao Y (2018) Lead and uranium sorptive removal from aqueous solution using magnetic and nonmagnetic fast pyrolysis rice husk biochars. RSC Adv 8:13205–13217

Wang Y, Kang J, Jiang S et al (2020) A composite of Ni–Fe–Zn layered double hydroxides/biochar for atrazine removal from aqueous solution. Biochar 2:455–464. https://doi.org/10.1007/s42773-020-00066-y

Wang B, Zhu C, Ai D, Fan Z (2021a) Activation of persulfate by green nano-zero-valent iron-loaded biochar for the removal of p-nitrophenol: performance, mechanism and variables effects. J Hazard Mater 417:126106

Wang WD, Ma HT, Lin W, Sun P, Zhang LK, Han JH (2021b) Trametes suaveolens-derived biochar loaded on nanoscale zero-valent iron particles for the adsorption and reduction of Cr (VI). Int J Environ Sci Technol 1:14

Wei D, Li B, Luo L, Zheng Y, Huang L, Zhang J, Yang Y, Huang H (2020) Simultaneous adsorption and oxidation of antimonite onto nano zero-valent iron sludge-based biochar: indispensable role of reactive oxygen species and redox-active moieties. J Hazard Mater 391:122057. https://doi.org/10.1016/j.jhazmat.2020.122057

Wen E, Yang X, Chen H, Shaheen SM, Sarka et al (2021) Iron-modified biochar and water management regime-induced changes in plant growth, enzyme activities, and phytoavailability of arsenic, cadmium and lead in a paddy soil. J Hazard Mater 407:124344

Wollenberg A, Kretzschmar J, Drobot B, Hübner R, Freitag L, Lehmann F, Günther A, Stumpf T, Raff J (2021) Uranium(VI) bioassociation by different fungi—a comparative study into molecular processes. J Hazard Mater 411:125068

Wu W, Li J, Lan T, Müller K, Niazi NK et al (2017) Unraveling sorption of lead in aqueous solutions by chemically modified biochar derived from coconut fiber: a microscopic and spectroscopic investigation. Sci Total Environ 576:766–774

Wu P, Ata-Ul-Karim ST, Singh BP et al (2019) A scientometric review of biochar research in the past 20 years (1998–2018). Biochar 1:23–43. https://doi.org/10.1007/s42773-019-00002-9

Wu H, Wei W, Xu C, Meng Y, Bai W, Yang W, Lin A (2020a) Polyethylene glycol-stabilized nano zero-valent iron supported by biochar for highly efficient removal of Cr(VI). Ecotoxicol Environ Saf 188:109902

Wu P, Wang Z, Wang H et al (2020b) Visualizing the emerging trends of biochar research and applications in 2019: a scientometric analysis and review. Biochar 2:135–150. https://doi.org/10.1007/s42773-020-00055-1

Wu P, Wang Z, Bolan NS et al (2021a) Visualizing the development trend and research frontiers of biochar in 2020: a scientometric perspective. Biochar 3:419–436. https://doi.org/10.1007/s42773-021-00120-3

Wu W, Han L, Nie X, Gu M, Li J, Chen M (2021b) Effects of multiple injections on the transport of CMC-nZVI in saturated sand columns. Sci Total Environ 784:147160

Wurzer C, Mašek O (2021) Feedstock doping using iron rich waste increases the pyrolysis gas yield and adsorption performance ofmagnetic biochar for emerging contaminants. Bioprocess Technol 321:124473

Xiong J, Zhou M, Qu C et al (2021) Quantitative analysis of Pb adsorption on sulfhydryl-modified biochar. Biochar 3:37–49. https://doi.org/10.1007/s42773-020-00077-9

Xu H, Gao M, Hu X, Chen Y, Li Y, Xu X, Zhang R, Yang X, Tang C, Hu X (2021) A novel preparation of S-nZVI and its high efficient removal of Cr(VI) in aqueous solution. J Hazard Mater 416:125924

Yan J, Han L, Gao W, Xue S, Chen M (2015) Biochar supported nanoscale zerovalent iron composite used as persulfate activator for removing trichloroethylene. Bioresour Technol 175:269–274. https://doi.org/10.1016/j.biortech.2014.10.103

Yang J, Zhao Y, Ma S, Zhu B, Zhang J, Zheng C (2016) Mercury removal by magnetic biochar derived from simultaneous activation and magnetization of sawdust. Environ Sci Technol 50:12040–12047

Yang C, Ge C, Li X, Li L, Wang B et al (2021a) Does soluble starch improve the removal of Cr(VI) by nZVI loaded on biochar? Ecotoxicol Environ Saf 208:111552

Yang F, Du Q, Sui L, Cheng K (2021b) One-step fabrication of artificial humic acid-functionalized colloid-like magnetic biochar for rapid heavy metal removal. Bioresour Technol 328:124825

Yang X, Pan H, Shaheen SM, Wang H, Rinklebe J (2021c) Immobilization of cadmium and lead using phosphorus-rich animal-derived and iron-modified plant-derived biochars under dynamic redox conditions in a paddy soil. Environ Int 156:106628

Yang X, Shaheen SM, Wang J, Hou D, Ok YS, Wang SL, Wang H, Rinklebe J (2022) Elucidating the redox-driven dynamic interactions between arsenic and iron-impregnated biochar in a paddy soil using geochemical and spectroscopic techniques. J Hazard Mater 422:126808

Yao S-h, Chen X-j, Gomez MA, Ma X-c, Wang H-b, Zang S-y (2020) One-step synthesis of zerovalent-iron–biochar composites to activate persulfate for phenol degradation. Water Sci Technol 80:1851–1860

Yi Y, Wang X, Ma J, Ning P (2020) An efficient Egeria najas-derived biochar supported nZVI composite for Cr(VI) removal: characterization and mechanism investigation based on visual MINTEQ model. Environ Res 189:109912

Younis SA, Kim K-H, Shaheen SM, Antoniadis V, Tsang YF, Rinklebe J, Deep A, Brown RJC (2021) Advancements of nanotechnologies in crop promotion and soil fertility: benefits, life cycle assessment, and legislation policies. Renew Sustain Energy Rev 152:111686

Yuan Y, Bolan N, Prévoteau A, Vithanage M, Biswas JK, Ok YS, Wang H (2017) Applications of biochar in redox-mediated reactions. Bioresour Technol 246:271–281

Zahedifar M, Seyedi N, Shafiei S, Basij M (2021) Surface-modified magnetic biochar: highly efficient adsorbents for removal of Pb(II) and Cd(II). Mater Chem Phys 271:124860

Zhang H, Ruan Y, Liang A, Shih K, Diao Z, Su M et al (2019a) Carbothermal reduction for preparing nZVI/BC to extract uranium: insight into the iron species dependent uranium adsorption behavior. J Clean Prod 239:117873

Zhang W, Wang H, Hu X, Feng H, Xiong W, Guo W, Zhou J, Mosa A, Peng Y (2019b) Multicavity triethylenetetramine-chitosan/

alginate composite beads for enhanced Cr (VI) removal. J Clean Prod 231:733–745

Zhang P, O'Connor D, Wang Y, Jiang L, Xia T, Wang L, Tsang DCW, Ok YS, Hou D (2020) A green biochar/iron oxide composite for methylene blue removal. J Hazard Mater 384:121286

Zhang Q, Wang Y, Wang Z, Zhang Z, Wang X, Yang Z (2021) Active biochar support nano zero-valent iron for efficient removal of U (VI) from sewage water. J Alloys Compd 852:156993

Zhao C, Hu L, Zhang C, Wang S, Wang X, Huo Z (2021) Preparation of biochar-interpenetrated iron-alginate hydrogel as a pH-independent sorbent for removal of Cr(VI) and Pb(II). Environ Pollut 287:117303

Zhou Y, Gao B, Zimmerman AR, Chen H, Zhang M, Cao X (2014) Biochar supported zerovalent iron for removal of various contaminants from aqueous solutions. Bioresour Technol 152:538–542

Zhou Y, Liu G, Liu J, Xiao Y, Wang T, Xue Y (2021) Magnetic biochar prepared by electromagnetic induction pyrolysis of cellulose: biochar characterization, mechanism of magnetization and adsorption removal of chromium (VI) from aqueous solution. Bioresour Technol 337:125429

Zhu L, Yin S, Yin Q, Wang H (2015) Biochar: a new promising catalyst support using methanation as a probe reaction. Energy Sci Eng 3:126–134

Zhu L, Tong L, Zhao N, Li J, Lv Y (2019) Coupling interaction between porous biochar and nano zero valent iron/nano α-hydroxyl iron oxide improves the remediation efficiency of cadmium in aqueous solution. Chemosphere 219:493–503

Zou Y, Wang X, Khan A, Wang P et al (2016) Environmental remediation and application of nanoscale zero-valent iron and its composites for the removal of heavy metal ions: a review. Environ Sci Technol 50(14):7290–7304

Zou H, Zhao J, He F, Zhong Z, Huang J, Zheng Y et al (2021) Ball milling biochar iron oxide composites for the removal of chromium (Cr(VI)) from water: performance and mechanisms. J Hazard Mater 413:125252